Role of Neisserial Outer Membrane Protein NhhA in Host-Pathogen Interaction

Master Thesis by Georg Philipp Altenbacher

Submitted in partial fulfillment of the requirements for the degree of Master of Science in Biochemistry and Molecular Biomedical Sciences at the Faculty of Technical Chemistry, Chemical & Process Engineering and Biotechnology at Graz University of Technology

Supervisor:	Prof. Dr. Peter Macheroux
	Institute of Biochemistry
	Graz University of Technology
Executive supervisor	Ass. Prof. Dr. Hong Sjölinder
	Department of Genetics, Microbiology and Toxicology
	Stockholm University

Graz/Stockholm 2011

EIDESSTATTLICHE ERKLÄRUNG

Ich erkläre an Eides statt, dass ich die vorliegende Arbeit selbstständig verfasst, andere als die angegebenen Quellen/Hilfsmittel nicht benutzt, und die den benutzten Quellen wörtlich und inhaltlich entnommene Stellen als solche kenntlich gemacht habe.

Graz, am ……………………………   …………………………………………………..

(Unterschrift)

Englische Fassung:

STATUTORY DECLARATION

I declare that I have authored this thesis independently, that I have not used other than the declared sources / resources, and that I have explicitly marked all material which has been quoted either literally or by content from the used sources.

……………………………   …………………………………………………..

date   (signature)

Acknowledgment

Firstly, I would like to thank Ass. Prof. Dr. Hong Sjölinder for giving me the unique opportunity to execute my master project as a member of her research group at Stockholm University and Prof. Dr. Peter Macheroux for his approval and for encouraging me to go abroad. Furthermore I want to thank Hong for her continuous support and for motivating me during the project.

Additionally, I want to express my deepest gratitude to Mikael Sjölinder, PhD, for his constant and never ending support, advises and help during the time we were designing, executing and discussing the experiments. I would not have made it without him.

Furthermore I would like to thank all lab members of the groups of Hong Sjölinder, Helena Aro, and Ann-Beth Jonsson for the good atmosphere, suggestions and help.

Last but not least, I want to thank my family for their support and for believing in me. Particularly my parents deserve to be mentioned separately for providing not only monetary aid but also a place where I am always welcome.

Abstract

N. meningitidis is a Gram-negative bacterium colonizing the human nasopahrynx. On some occasions, meningococci cross cellular barriers and enter the blood stream or the cerebrospinal fluid where they cause devastating diseases like sepsis and meningitis. Several virulence factors of *N. meningitidis* are involved in these processes. This work will focus on the neisserial outer membrane protein NhhA. It has been shown that NhhA plays a crucial role in colonizing hosts and in bacterial survival in the bloodstream. NhhA is an autotransporter protein comprising a passenger domain and a translocator domain. In the following studies, NhhA-FL a his-tagged truncated version of NhhA, consisting only of the mature passenger domain, is used.

Results indicate that NhhA-FL induces apoptosis in RAW264.7 and THP-1 cells. Additionally it is shown that induction of apoptosis is significantly decreased by a *nhhA* deficient FAM20 strain. Furthermore it is shown that NhhA-FL has a remarkable high potential of inducing elevated expression of proinflammatory cytokines such as Il6 and TNFα. Moreover upregulation of mRNAs encoding for other cytokines, particularly Csf3, Il1b, Il6, Csf2, Il1a, Ptgs2, Il10, Ccl2, Ifnb1, Cxcl10 and TNFα in RAW264.7 cells was observed. These results were confirmed in differentiated THP-1 cells with the cytokines Csf3, Il1b, Il6, Csf2, Il1a and TNFα.

In conclusion, these results indicate an apoptotic and a strong inflammatory potential of NhhA-FL.

Zusammenfassung

N. meningitidis ist ein Gram-negatives Bakterium und kolonisiert die menschliche Nasopharynx. Unter besonderen Umständen können Meningokokken zelluläre Barrieren überwinden und in den Blutkreislauf oder in die zerebrospinale Flüssigkeit gelangen. Dort verursachen sie verheerende Krankheiten wie zum Beispiel Sepsis und Meningitis. Diverse Virulenzfaktoren von *N. meningitidis* sind dabei involviert. Der Schwerpunkt dieser Arbeit liegt auf dem neisserialen Protein NhhA, lokalisiert in der äußeren Membran. Es wurde bereits gezeigt, dass NhhA eine entscheidende Rolle in der Kolonisierung von Wirten und im Überleben des Bakteriums im Blutkreislauf spielt. NhhA gehört zu den Autotransporterproteinen und besteht aus einer Passagierdomäne und einer Translokationsdomäne. In den folgenden Studien wird NhhA-FL verwendet. Dies ist eine his-markierte, abgeschnittene Version von NhhA und besteht nur aus der reifen Passagierdomäne.

Die folgenden Resultate zeigen, dass NhhA-FL Apoptose in RAW264.7 und THP-1 Zellen auslöst. Weiters zeigen sie, dass der Bakterienstamm FAM20 mit fehlendem *nhhA* Gen ein signifikant geringeres Apoptosepotential hat. Außerdem hat NhhA-FL ein außerordentlich hohes Potential, die Ausschüttung proinflammatorischer Zytokine, wie zum Beispiel Il6 und TNFα, zu induzieren. Die mRNAs, insbesondere die Csf3, Il1b, Il6, Csf2, Il1a, Ptgs2, Il10, Ccl2, Ifnb1, Cxcl10 und TNFα kodieren, werden in RAW264.7 Zellen nach NhhA-FL Behandlung erhöht exprimiert. Diese Resultate wurden in differenzierten THP-1 Zellen mit Csf3, Il1b, Il6, Csf2, Il1a und TNFα bestätigt.

Zusammenfassend kann man sagen, dass diese Resultate auf ein hohes apoptotisches und inflammatorisches Potential von NhhA-FL hindeuten.

Abbreviations

AA/Bis	acrylamide/N,N'-methylenebisacrylamide
CD	cluster of differentiation
CMP-NANA	cytidine-5'-monophospho-NANA
E. coli	*Escherichia coli*
EDTA	ethylenediaminetetraacetate
ELISA	enzyme linked immunosorbent assay
f. c.	final concentration
GC	chocolate broth
h	hour
his	histidine
HSPG	heparan sulfate proteoglycan
Il	interleukin
kDa	kilo dalton
KDO	2-keto-3-deoxy-D-manno-2-octulosonic acid
LB	lysogeny broth
LBA	lysogeny broth supplemented with ampicillin
LNnT	lacto-N-neotetraose
LOS	lipooligosaccharides
MOI	multiplicity of infection
MyD88	myeloid differentiation primary response gene 88
N. meningitidis	*Neisseria meningitidis*
NANA	5-N-acetylneuraminic acid
OD_{600}	optical density at a wavelength of $\lambda=600$ nm
page	polyacrylamide gel electrophoresis
PMA	phorbol 12-myristate 13-acetate
SDS	sodium dodecyl sulfate
TAE	tris acetic acid EDTA
TBE	tris borate EDTA
TEMED	N, N, N', N'-tetramethlethylenediamine
TLR	Toll-like receptor
TNFα	tumor necrosis factor α
Tris	2-amino-2-(hydroxymethyl)propane-1,3-diol
V	Volt

Index

1. Introduction

1.1. Neisseria meningitidis

Neisseria meningitidis belongs, together with *N. gonorrhoeae*, to the genus *Neisseria*. It is a human-specific, Gram-negative bacterium, which often occurs in diplococcal form. *N. meningitidis* is the leading cause of bacterial meningitis worldwide. Even Austria is not a safe place, as the case of an outbreak with lethal outcome in April 2011 demonstrates. The sole ecological niche of *N. meningitidis* is the human nasopharynx. The main difference between *N. meningitidis* and *N. gonorrhoeae*, besides the habitat, is the expression of a polysaccharide capsule of *N. meningitidis*. This is also the basis of the classification of *N. meningitidis* into serogroups. Depending on the composition of this capsule, 13 different serogroups have been defined. Six of this serogroups, namely A, B, C, W-135, X and Y, cause most of the life threatening diseases (*1-4*).

1.1.1. Epidemiology, carriage and disease

Five to ten percent of adults carry meningococci asymptomatically during nonepidemic periods in their nasopharynx. Transmission happens through droplet transfer during either direct contact with nasal or oral secretions or by inhalation (*5*). Meningococcal disease varies in incidence and may increase to over 1000 cases per 100000 population. Serogroup A is the group, which causes most diseases. In particular sub Saharan areas are most affected by pandemics caused by *N. meningitidis* serogroup A but serogroup C also plays an important role. This area is therefore, called the African meningitis belt, it spreads from Ethiopia in the east to Senegal in the west. In Europe and America diseases are predominantly caused by serogroups B and C, W-135 is responsible for outbreaks worldwide, whereas Y is associated with diseases in the U.S.A and Canada (*1*, *3*, *6*).

As mentioned before, five to ten percent of all adults are carriers. Nevertheless, this fact highly depends on the social environment. The carriage rate could approach 100 % in individuals with close contact to each other like military recruits or students, especially in their freshmen year. This is also associated with age as one of the most important impact factors on the carriage rate in European and North American countries. In these countries carriage rate is low in the first years of life. It increases in teenagers and reaches its climax in people at the age of 20 to 24. Predispositions for developing invasive disease are for instance smoking, low humidity and drying out of the mucosal surface and, most important, lack or deficiency of antibody dependent

complement-mediated immune lysis (*1-3*, *6*). In accordance to this, a big study of the social behavior and meningococcal carriage in teenagers revealed that the rise in carriage is driven by changes of social behavior. It was shown that attendance of pubs or clubs, intimate kissing and cigarette smoking were strongly associated with meningococcal carriage (*7*).

Mortality occurs in approximately 10 % of patients, but this strongly depends on the type of invasive disease. Mortality reaches 55 % in patients with fulminant septicemia and 25 % in patients with meningitis with associated septicemia. Lowest mortality rates, namely below 5 %, are observed for meningitis alone. Survivors often suffer from severe physical and mental sequelae (*1*).

1.1.2. Virulence factors

Particularly the outer membrane of *N. meningitidis,* which contains capsular polysaccharides, lipopolysaccharides (LPS), pili and other proteins, most important Opa, Opc, PorA and PorB, contributes remarkably to the virulence (*5*).

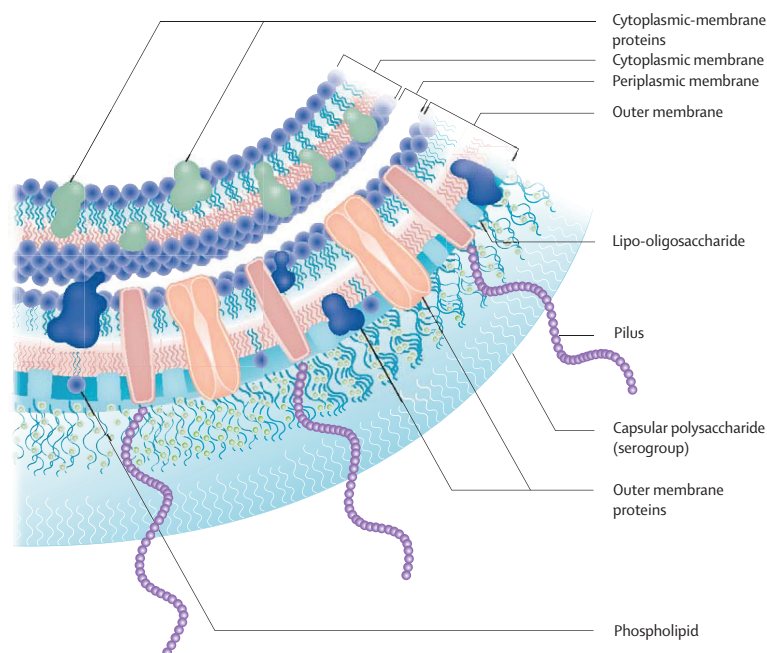**Fig. 1: Cross-section of the meningococcal membrane** (*3*)**.**

Capsule

When *N. meningitidis* is isolated from carriers it may be capsulated or acapsulated in contrast to isolates from blood or cerebrospinal fluid (CNF) where *N. meningitidis* is always capsulated. This indicates that the capsule is crucial for the survival of meningococci in blood. In general, the capsule prevents antibody and complement-

mediated killing and inhibits opsonic and non-opsonic phagocytosis (*1*). Additionally, the capsule provides the meningococcus with a protection against desiccation and antiadherent properties, both contribute to the promotion of transmission (*5*).

Capsular genes are located on the chromosomal locus *cps*, which is divided into three regions, namely A, B and C (*1*). *cps* was previously divided into 5 regions (A, B, C, D and E), but the latter two regions have regulatory functions only since mutation in these regions does not affect polysaccharide synthesis or translocation. All serogroups associated with invasive diseases, except serogroup A, contain sialic acid in their capsule. Genes encoded on region A seem to be essential for synthesizing and polymerizing this 5-N-acetylneuraminic acid (NANA). Regions B and C code for genes which are involved in translocation of capsular polysaccharides to the periplasm and the outer membrane, respectively (*1*, *8*). The *cps* region A of serogroups expressing sialic acids harbors four conserved genes, namely *siaA, siaB siaC*, involved in NANA synthesis in the form of cytidine-5'-monophospho-NANA (CMP-NANA), and *siaD*, which encodes for a serogroup-specific polysialyltransferase involved in polymerization and, therefore, specifying the serogroup (*1*). The capsule of serogroup A *N. meningitidis* consists of (α1→6)-linked N-acetyl-D-mannosamine-1-phosphate, nevertheless, the genomic organization of the genes involved in capsule synthesis and translocation of is similar to the one of the other serogroups. Instead of the *siaA* to *siaD* genes, *cps* contains *mynA* to *myn*D genes. *mynA* encodes for the epimerase converting uridine diphosphate N-acetylglucosamine to uridine diphosphate N-acetyl-D-mannosamine, *mynB* encodes for the protein responsible for polymerization and *mynC* and *mynD* are involved in further modifications (*1*, *9*).

Additionally to *N. meningitidis'* mimicry of host cells due to the incorporation of sialic acid into the capsule, capsule switching has also been reported. The genetic similarities in serogroups expressing sialic acid in the *cps* and the natural competence of *N. meningitidis* favors horizontal exchange of proteins of the capsule biosynthetic operon between serogroups. This serves as a mechanism to escape from vaccine-induced or natural protective immunity. It is noteworthy that this could become even more important with the widespread use of serogroup specific vaccines, which could lead to an increased switching of capsule to serogroup B, against which no vaccine is available. Nevertheless, significant immunization-associated capsule switching has not been observed yet (*1*, *3*, *6*).

Lipooligosaccharides LOS

Owing to the lack of repeating O antigen units and shorter polysaccharide chains, meningococcal lipopolysaccharides are also known as lipooligosaccharides. LOSs, or endotoxins, seem to be the most potent but not the sole inducer of inflammatory responses, particularly the proinflammatory cytokines and chemokines like interleukin 1 (Il1), Il6 and tumor necrosis factor (TNF) are highly upregulated upon LOS stimulation (*10, 11*). The overall structure of LOS is always the same: the inner core structure consists of diheptoses (HepI and HepII) attached to lipid A via one of the two 2-keto-3-deoxy-D-manno-2-octulosonic acids (KDO). This core structure is substituted by short polysaccharide chains at the HepI and HepII positions. The α-chain is attached to HepI and the β-chain is attached to HepII which itself is attached to HepI. LOS is variable due to phase variation and slipped strand mispairing. These effects lead to antigenic variations and, as a consequence, to a classification into 12 different immunotypes. One strain can express several different immunotypes, nevertheless, one immunotype is usually dominant. The *lst* gene for instance is responsible for terminal galactose binding giving rise to the L3 immunotype. *lgt* genes encode for glycosyltransferases, which add sugars to the α- and β-chain. Phosphoethanolamine (PEA) can be added by *lpt6* and *lpt3* at positions 6 or 3 of HepII, respectively (*1, 10, 12*). In some of these immunotypes lacto-N-neotetraose (LNnT) is detected, particularly in virulent strains of *N. meningitidis.* LNnT serves as an acceptor for sialic acid, which is produced in serogroups B, C, W-135 and Y as mentioned before. Serogroups, which do not produce CMP-NANA, such as serogroup A strains, acquire sialic acid from exogenous sources. This may also contribute to immune evasion. (*1*).
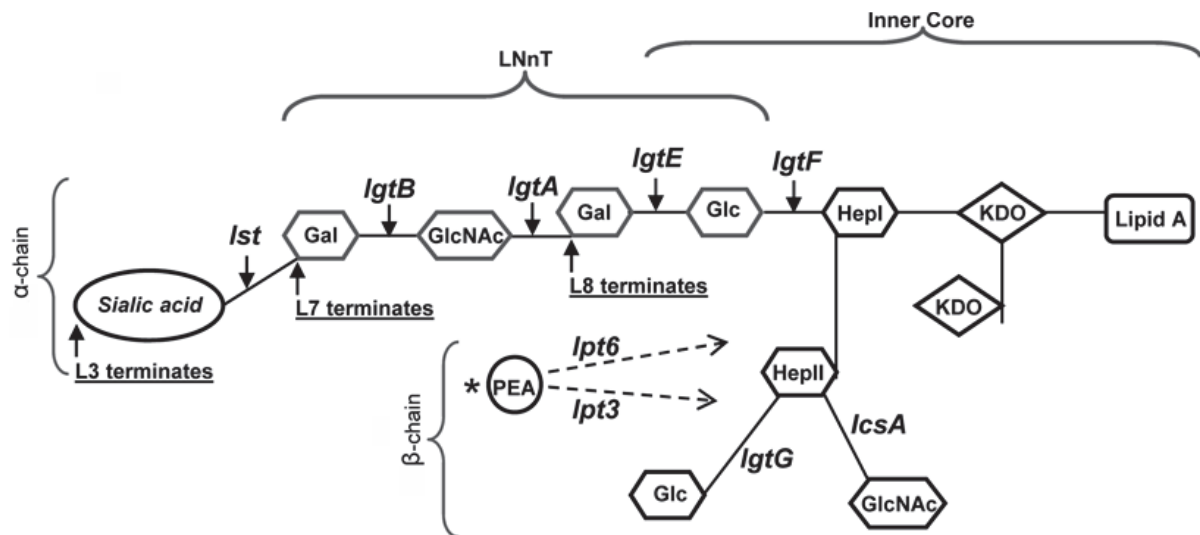
Fig. 2: Schematic diagram showing a meningococcal LOS immunotype with LNnT. PAE: phosphoethanolamine; Gal: galactose; Glc: glucose; GlcNAc: N-acetylglucosamine (*1*).

It is commonly known that endotoxin release requires at least lysis of bacteria. Additionally meningococci release LOS as cell wall blebs during log-phase growth (*13*). It has been shown that LOS induces the inflammatory response due to signaling via the cluster of differentiation (CD) 14/Toll-like receptor 4 (TLR4)–lymphocyte antigen 96 (MD-2) receptor pathway. Inhibiting CD14 reduces TNFα release and inhibition of TLR4 reduces cytokine release in general. Additionally, the structure of the α- and β-chain has no influence on CD14/TLR4–MD-2 receptor activation but linking of the KDOs to the lipid A is required (*14*). Further downstream LOS stimuli are transduced via the myeloid differentiation primary response gene 88 (MyD88)-dependent and –independent pathway. This is quite remarkable for LOS since lipopolysaccharides from other organisms usually induce more selectively (*15*).

Pili

Meningococcal pili belong to the most widespread type IV family. Type IV pili are the only type found on Gram-positive and Gram-negative bacteria, therefore, suggested to be the most widespread organ of bacterial attachment. In *N. meningitidis* type IV pili is supposed to be the most important adhesion factor. Type IV pili are very thin, around 6 nm in diameter, but several micrometers long. They are flexible and aggregate laterally to form bundles (*1, 16*). 15 genes located on various positions on the genome are responsible for pilus biogenesis, which can be distinguished in assembly, functional maturation, emergence on the cell surface and counter-

retraction (*17*). The major subunit of neisserial pili is the pilin, encoded by *pilE*. Pilin is synthesized as a preprotein and cleaved by PilD. *pilS* are silent, truncated copies of *pilE* and serve as a source of variation, leading to new PilE variants. PilG is located at the inner membrane and required for piliation due to its capability of preventing pilus retraction. Nevertheless, like PilT it is not required for pilus biogenesis. PilT and PilF are both ATPases associated to the inner membrane. While PilF is responsible for pilus elongation, and, therefore, also required for biogenesis, PilT is responsible for pilus retraction. PilQ is localized in the outer membrane and supports extrusion and retraction of the pili and targets the laminin receptor as an adhesion. It consists of 12 identical monomers. Two types of PilC proteins exist in *N. meningitidis* but only PilC1 is required for adhesion. Several other prepilin like proteins with pilin-like N-terminal sequences exist, which are cleaved by PilD. For instance, ComP and PilV are responsible for DNA transformation and adhesion to human cells, respectively. PilX is involved in bacterial aggregation and adhesion (*17*, *18*).
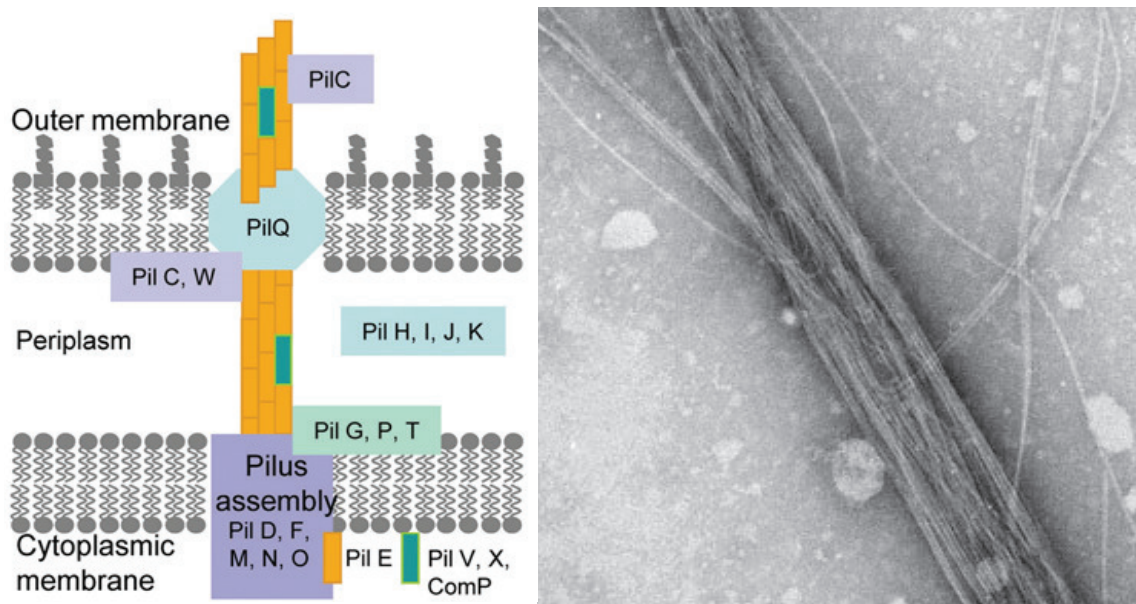

Fig. 3: Left: scheme of a pilus (*1*)**; right: transmission electron microscopy picture of a pili bundle of *N. meningitidis*** (*16*)**.**

CD46 was considered to be the major cellular receptor for type IV pili of *Neisseria* but recent evidence suggests, that CD46 is not the only receptor responsible for type IV pili interaction with host cells. Nevertheless, in conclusion, type IV pili are responsible for adhesion, twitching motility, due to pilus elongation and retraction, and for the natural competence of *N. meningitidis* (*5*, *17*, *19*, *20*).

Opacity proteins

Opa and Opc belong to the opacity proteins, they have a size between 24 and 35 kDa and share many features although their corresponding genes and predicted two-dimensional structures are unrelated. Opa and Opc were previously termed as class 5 proteins. Opa is also expressed in *N. gonorrhoeae* and is responsible for the opaque appearance in agar-grown colonies. In *N. meningitidis* the opaque phenotype is not visible due to the capsule. Opc is only expressed in meningococci (*1, 17, 21*).

The Opa protein is encoded by three to four *opa* loci, which can be expressed independently from each other. Additionally, the *opa* gene contains tandem CTCTT repeats, which determine whether the gene is in frame or not. Furthermore, these repeats contribute to frequent phase variation due to slipped strand mispairing. Nevertheless, the major antigenic variations arise from changing the expression form one *opa* gene to the other (*1, 17*).

The Opa protein consists of eight transmembrane β-strands and thus forms a β-barrel in the outer membrane. This results in the presentation of four hydrophilic loops on the cell surface and in termination at the inner face of the outer membrane. The first three loops are highly variable in sequence and called semivariable (SV), hypervariable (HV) 1 and HV2. The other parts of the protein are considered as a conserved framework (*22*).

The Opc protein (OpcA) is a 10-stranded β-barrel encoded by a single gene. It is rather invariant and the expression levels vary due to a transcriptional control mechanism. Several strain expressing OpcA cause septicemia but are less associated with meningitis. The reason for that could be related to OpcA (*17*).

Opa proteins bind different members of the carcinoembryonic antigen-related cell adhesion molecules (CEACAMs). Since the expression of these receptors is restricted to particular cells or tissue it imparts tissue tropism to *N. meningitidis.* Opc on the other hand interacts with the serum glycoprotein vitronectin and attaches to integrins, which are present on the surfaces of endothelial cells. Additionally both, Opa and Opc, bind to heparan sulfate proteoglycans and sialic acids (*17, 21, 23-25*).

Porins

The two porins expressed by *N. meningitidis* are PorA and PorB. The structure of neisserial porins is trimeric, each of the polypeptides is around 35 kDa large and consists to approximately 36% of β-pleated sheets. Therefore, the predicted structure is a β-pleated-barrel. Porins function as pores as they modulate the exchange of ions.

Additionally, they can be inserted into eukaryotic target cell membranes where they form transmembrane channels, change the membrane potential and interfere with cell signaling. On the other hand, human opsonins and bactericidal antibodies recognize these two outer membrane proteins (*5, 26, 27*).

Proins also influence apoptosis of the host cell though conflicting data has been reported. On the one hand, it has been shown, that PorB induces apoptosis due to a transient increase of cytosolic Ca^{2+} and subsequent activation of calpain and caspases. Additionally, the porin is transported to mitochondria and prevention of this translocation blocked induction of apoptosis. On the other hand, it has been shown that pretreatment with meningococcal PorB decrease mitochondrial damage induced by apoptotic stimuli. PorB interacts with the mitochondrial porin voltage-dependent anion channel (VDAC) in a similar way as antiapoptotic Bcl-2 proteins do. This enhanced survival. It is noteworthy that the results showing pro-apoptotic effects were obtained from gonococcal PorB and the results showing anti-apoptotic effect from meningococcal PorB (*28-31*).

1.1.3. Colonization and crossing of epithelial barriers

Colonization

To be able to colonize a host, *N. meningitidis* has to adhere to the epithelial surface of the nasopharynx. In this step, type IV pili are most important mediators of adhesion. As mentioned before, CD46 is considered to be the receptor despite recent evidence of CD46-independent adhesion (*19, 20, 32*). Initially, *N. meningitidis* forms microcolonies on cell surfaces due to three-dimensional growth and induces changes in the host. For instance, formation of cortical plaques is induced by the recruitment of cholesterol. These plaques contain CD44v3, which is a heparan sulfate proteoglycan (HSPG), the receptor tyrosine kinase epidermal growth factor receptor (EGFR), CD44 and inter-cellular adhesion molecule 1 (ICAM-1), both are adhesion molecules and mediate inflammatory responses, f-actin, moesin and ezrin, which links membrane components to the actin cytoskeleton. Additionally, meningococcal microcolonies induce cellular projections, similar to microvilli, which protrude into the microcolony and protect it from shear stress (*32-35*). After this initial adhesion it is essential for meningococci to disperse on the apical cell surface and to downregulate type IV pili and the capsule to ensure a more stable adhesion to the cell surface for a long-term colonization. This more intimate adhesion is

maintained by other outer membrane proteins like opacity proteins, LOS and several others like NadA and NhhA (*24*, *32*, *36*, *37*).

Crossing cellular barriers – entering the blood stream and the cerebrospinal fluid

During certain conditions, meningococci are able to cross epithelial cell barriers via a transcellular route. Important for this to occur is the expression of type IV pili and the capsule. The capsule is needed for bacterial survival in the blood, therefore, it is important not to mix up the requirements for long-term colonization with the ones for invasion (see above). Internalization happens after dispersal and retraction of the pili. It has been shown that *N. meningitidis* crosses epithelial barriers established with Calu-3 cells grown in a monolayer on a 1-µm membrane via a transcellular route. This *in vitro* model resembles a respiratory epithelial barrier (*37*).

Additionally, Eugène et al. have shown that the microvilli like structures, which also assist in protection of shear stress (see above), are involved in internalization into endothelial cells, which is associated with meningeal invasion (*35*).

1.1.4. Clinical representation, prevention and treatment

The symptoms of meningococcal induced septicemia are mostly fever and petechial or purpuric rash associated with rapid onset of hypotension, ecchymoses, sometimes red maculae with a diameter greater than 1 cm, acute adrenal hemorrhage and multiorgan failure. Meningeal infections are mostly represented with fever, headache and stiffness of the neck. Additionally, nausea, vomiting, photophobia and an altered mental status could occur. In general, the symptoms are similar to less severe illnesses and, therefore, difficult to distinguish. Another important thing is that the preliminary symptoms such as leg-pain, cold hands and feet or an abnormal skin color are often underestimated and not associated with meningococcal infection by parents and, therefore, seldom reported despite the possible importance of these symptoms (*3*, *6*, *38*).
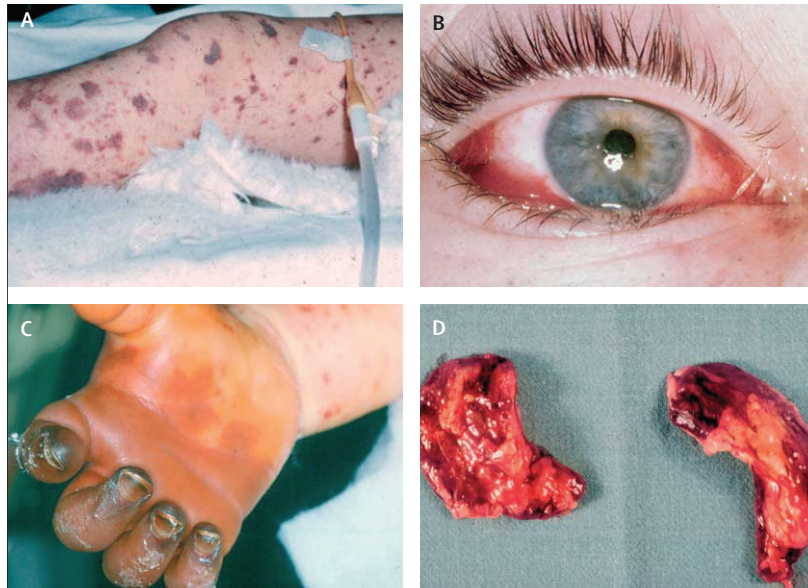
Fig. 4: (A) ecchymoses, (B) intraocular hemorrhage, (C) thrombosis and gangrene, (D) hemorrhagic adrenals, all caused by fulminant meningococcal septicemia (*3*)

Treatment is always parenteral administration of β-lactam antibiotics like penicillins and cephalosporins. Although the sensitivity of meningococci to benzylpenicillin is decreasing, high-level penicillin resistances are rare. Antibiotics should be administered as soon as possible, even prehospital antibiotic treatment is advised. The time window for treatment closes very soon since meningococci have a doubling time of only 30 to 45 minutes (*1*, *3*, *6*).

One of the biggest problems with meningococcal infections is the fast onset of disease. Therefore, preventive techniques are applied. For instance, chemoprophylaxis is used to eliminate meningococci from carriers. This is a useful method to control localized outbreaks, particularly in schools, barracks or similar (*3*, *6*).

Additionally, quadrivalent polysaccharide vaccines for serogroups A, C, W-135 and Y exist. These induce good immunogenicity particularly for serogroups A and C but antibodies against serogroups Y and W-135 are also detected in vaccinated humans. The clinical efficacy rates are above 85% in children older than five years (in some reports, older than two years). One of the biggest problems with this vaccine is that it does not induce an immunological memory. Routine childhood vaccination with this quadrivalent vaccine is not recommended due to ineffectiveness in young children. No serogroup B vaccine is currently available although local effective vaccines have been developed and clinically tested. Sub-capsular vaccines, particularly outer membrane vesicle vaccines, have also been successful against some hyperinvasive

lineages. Nevertheless this is currently further investigated by researchers to develop a vaccine which is effective against a broad range of meningococci (*1-3*, *6*)

1.2. Neisserial Hia/Hsf homologue

The sequence of NhhA, also termed GNA0992, in *N. meningitidis* was reported and patented by Michael P. Jennings et al.. Sequence homology to the adhesions AIDA-I of *E. coli* and Hia and Hsf of *H. influence* are also reported. NhhA belongs to the class of autotransporters (*36*, *39-41*).

nhhA exhibits 89.5-99.8% sequence similarity in different *N. meningitidis* strains and the open reading frames range from 1770 to 1800 bp. This results in a predicted protein of 589-599 amino acids. The highest variable region is between amino acid 51 and 250, which resemble the first 200 amino acids of the mature protein. 93% of the amino acid residues outside of this region are conserved. It has been shown that *nhhA* is present in a vast majority of disease associated strains of *N. meningitidis*. NhhA is accessible to antibodies and, therefore, surface exposed. Additionally, in humans recovering from meningococcal diseases detection of anti-NhhA antibodies is possible indicating that NhhA is immunogenic in humans (*36*, *40*, *41*).

The following figure shows a functional mapping of NhhA in the strain 2996 of *N. meningitidis* (*36*):
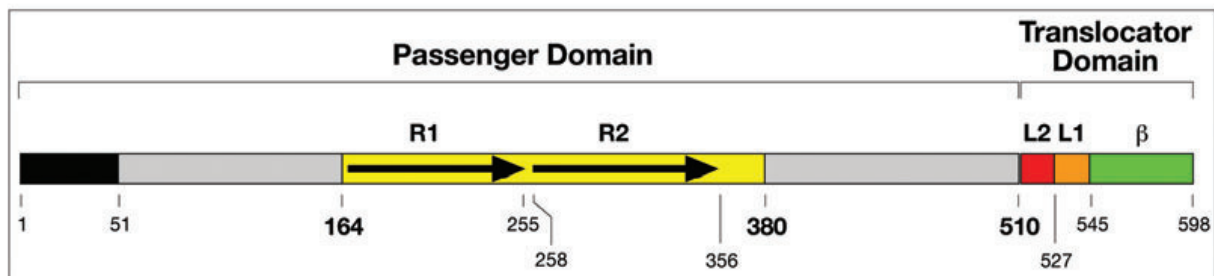

Fig. 5: *In silico* **functional mapping of NhhA** (*36*)

NhhA comprises three big regions, the first is the leading peptide from amino acid 1 to 51, secondly the passenger domain, which is homologous to Hia/Hsf and reaches from amino acid 52 to 509 and finally the translocator domain from amino acid 510 to 598. The passenger domain reaches into the extracellular space and interacts with the environment. The N-terminal region starting with amino acid 51 to amino acid 163 shows 81% identity to Hsf. The region from amino acid 164 to 380 shows 69.3% identity to Hia and a variable similarity of 53.5 to 66.2% to Hsf. Additionally, this region contains two modules called R1 and R2, which hold a predicted binding site for heparan-sulphate. Conclusively HSPG and laminin binding has been reported.

Region 381 to 509 shows least identity to Hia and Hsf and, therefore, contributes to the functional specificity of NhhA. The C-terminal region is the translocator domain and starts with amino acid 510. This domain is responsible for trimerizing and insertion into the outer membrane. It is divided into the L2, L1 and β regions but several results suggest that the L1 and β region are sufficient for trimerizing and exporting the passenger domain. The following figure shows a putative 3D structure of the translocation domain (*36*, *42*).
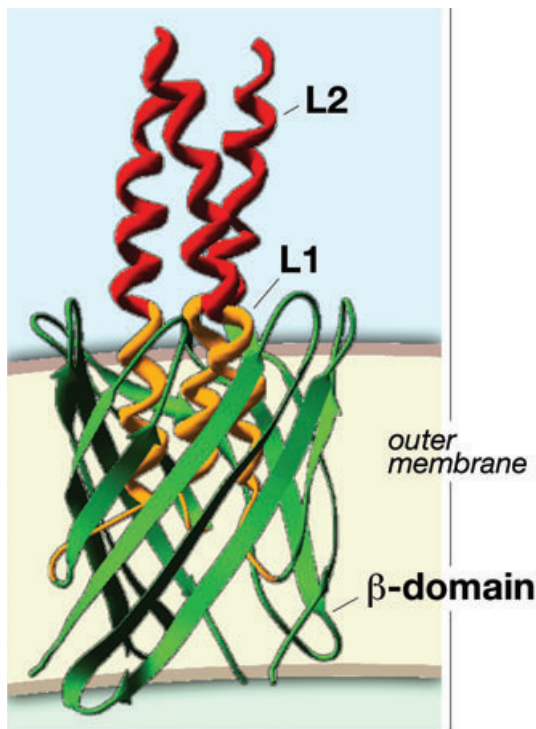
Fig. 6: Putative structure of the translocator domain generated with the DeepView/Swiss-Pdb viewer (*36*).

NhhA is particularly biologically relevant in adhesion to epithelial cells, protecting bacteria from phagocytosis and serum resistance. Therefore, NhhA is not only involved in colonization but also in the development of sepsis (*36*, *43*). It has been shown that *nhhA* deficient mutants of *N. meningitidis* are not as potent in adhering to epithelial cells. Additionally, *E. coli* expressing NhhA were able to interact with epithelial cell lines (*36*). A different study using a transgenic CD46 mouse model showed consistent results. Mice were challenged with either *N. meningitidis* FAM20 or the FAM20ΔnhhA mutant and results showed neither lethal outcome nor bacteremia in mice treated with the mutant strain in contrast to mice treated with the wild type strain. 15% of the mice infected with the wild type died in contrast to none of the ones treated with the *nhhA* deficient mutant. In the same study it was shown that FAM20ΔnhhAs ability to survive intracellularly in mouse macrophages was decreased. Mice *intra peritoneally* infected with FAM20ΔnhhA show increased

survival compared to mice infected with wild type bacteria. Additionally, bacterial survival of the mutant strain markedly decreased when treated with normal human serum compared to the wild type. Further analysis subsequently showed that the FAM20ΔnhhA is more accessible to binding of the membrane attack complex (*43*).

1.3. Aim of this master project

The primary goal was to investigate further properties of NhhA. In particular, the influence on apoptosis induction in macrophages and the proinflammatory potential of NhhA was investigated. We also wanted to get a closer look on the signal cascade, which is responsible for upregulation of proinflammatory cytokines. Previous results suggested a pathway via NFκB and the Toll-like receptor pathways but the exact details remained unclear (unpublished data). Additionally, we wanted to compare the proinflammatory potential of NhhA with other virulence factors, especially LOS as one of the most important inducers of proinflammatory cytokines (*10*, *11*). Moreover, we also tried to assess which part of NhhA is necessary for induction of cytokine release.

All this data will help to get a better understanding of NhhAs involvement into host-bacteria interaction. Furthermore, it will contribute to the general understanding of how external molecules affect cells in terms of signal transduction. Ultimately, if a distinct pattern of induction of proinflammatory cytokines between the protein fragments is found, it will be beneficial for developing vaccines or treatment therapies.

2. Materials and Methods

2.1. Materials

Chemicals and kits:

Standard chemicals unless otherwise indicated	Sigma Aldrich, VWR, Merck
1 kb DNA Ladder	Fermentas
100 bp DNA Ladder	Fermentas
10x buffer for T4 DNA ligase	Fermentas
10x Fast Digest Buffer	Fermentas
10x FastAP Buffer	Fermentas
10x TBE Buffer	Bio-Rad
AccuGene 10x PBS	Lonza
Adv. DMEM	Gibco™-Invitrogen
Antibiotic-Antimycotic (100x PeSt)	Gibco™-Invitrogen
APOPercentage Apoptosis Assay	biocolor
Bradford reagent	Bio-Rad
CLI-095	Invivogen
DMEM	Gibco™-Invitrogen
E.Z.N.A.™ Cycle-Pure Kit	Omega Bio-Tek
E.Z.N.A.™ Plasmid Miniprep Kit I	Omega Bio-Tek
ELISA MAX™ Standard Set Mouse TNFα	BioLegend
Fast Digest BamHI	Fermentas
Fast Digest HindIII	Fermentas
FastAP	Fermentas
FBS	Gibco™-Invitrogen
Glutamax	Gibco™-Invitrogen
High Fidelity DNA Polymerase Kit	Finnzymes
HiPerFect® Transfection Reagent	Qiagen
LightCycler 480 SYBR Green I Master	Roche Diagnostics
Maxima SYBR Green/ROX qPCR Master Mix (2x)	Fermentas
Mouse IL-6 Antibody Pair	Invitrogen™
Mouse TNFα Antibody Pair	Invitrogen™

Murine IL-6 ELI-Pair	GEN-PROBE-Diaclone
PageRuler™ Prestained Protein Ladder	Fermentas
Pam3CSK4	Invivogen
pET21a	Novagen
Phorbol 12-myristate 13-acetate (PMA)	Fisher Scientific
Proteinase K, 20 mg/mL	Fermentas
Revert Aid H minus First Strand cDNA Synthesis Kit	Fermentas
RNase-Free DNase Set (50)	Qiagen
RNeasy® Mini Kit	Qiagen
RPMI 1640	PAA
RT^2 First Strand Kit	SABiosciences
RT^2 SYBR Green qPCR Master Mix	SABiosciences
RT^2 Toll-Like Receptor Signalling Pathway PCR Array	SABiosciences
T4 ligase	Fermentas
Talon® Metal Affinity Resin	Clontech
λ/HindIII DNA Ladder	Fermentas

Equipment:

Agarose gel documentation system	Gel Doc 2000, Bio-Rad
Centrifugal filter units	Amicon® Ultra Centrifugal Filters 10000 MWCO, Millipore
Centrifuges	Heraeus Pico 21, Thermo-Scientific Heraeus Labfuge 400R, Thermo-Scientific
Columns for protein purification	Econo-Column®, Bio-Rad
DNA electrophoresis equipment	Mini-Sub® Cell GT, Bio-Rad
Electrophoresis power supplies	PowerPac™ Basic, Bio-Rad PowerPac™ HC, Bio-Rad
Filter for flow cytometry	30 µm Cup-Filcons, BD Biosciences
Flow cytometer	LSRFortessa™, BD
Flow cytometer tubes	5 mL Polystyrene Round-Bottom-Tube, BD Falcon™
Microscope	Axiovert 40 C, Zeiss

PCR devices	Piko Thermal Cycler, Finnzymes
	LightCycler® 480 II, Roche Diagnostics
Plasticware (multiwell plates, serological pipettes, T-bottles, 15 mL and 50 mL tubes, cell scraper, syringes)	Costar®-Corning®, Falcon®-Becton Dickinson, Sarstedt, BD Plastipak™
SDS-PAGE equipment	Mini PROTEAN® Tetra Cell, Bio-Rad
Sonicator	sonicator® ultrasonic processor XL, Misonix
Spectrophotometers	Nanodrop® ND-8000, Thermo-Scientific SmartSpec™ Plus, Bio-Rad
Syringe filters	Filtropur S 0.2, Sarstedt
Western blot documentation system	Odyssey®, LiCor® Biosciences
Western blot membrane	PVDF-Plus transfer membrane, SantaCruz

siRNAs:

AllStar n. c.	AllStar negative control siRNA, Qiagen
CD14_1	siRNA against mouse CD14, Qiagen
CD14_2	siRNA against mouse CD14, Qiagen
MyD88_2	siRNA against mouse MyD88, Qiagen
MyD88_4	siRNA against mouse MyD88, Qiagen
TLR1_1	siRNA against mouse TLR1, Qiagen
TLR1_7	siRNA against mouse TLR1, Qiagen
TLR2_1	siRNA against mouse TLR2, Qiagen
TLR2_2	siRNA against mouse TLR2, Qiagen

Bacterial strains and cell lines:

BL21(DE3)	Invitrogen™
BL21(DE3)+NhhA-FL	BL21(DE3) *E. coli* expressing His-tagged NhhA protein without the leading peptide and the translocator domain; provided by A. Prof. Dr. Hong Sjölinder
FAM20	*N. meningitidis* serogroup C strain
FAM20ΔnhhA	*N. meningitidis* without the *nhhA* gene;

One Shot® TOP10 competent cells	provided by A. Prof. Dr. Hong Sjölinder Invitrogen™
RAW264.7	ATCC® number: TIB-71™; mouse cell line
THP-1	ATCC® number: TIB-202™; human cell line

Antibodies:

Mouse anti NhhA serum	Provided by Dr. Jafar Mahdavi, BSc, PhD, University of Nottingham
680-donkey anti mouse IgG 0.5 mg	LiCor, Kat. # 926-32222

Growth Media:

GC media:	15 g/L protease peptone no. 3 (Oxid), 1 g/L starch , 4 g/L K_2HPO_4, 1 g/L KH_2PO_4, 5 g/L NaCl
GC plates:	36 g/L GC agar (accumedia®), 10 mL Kellogg's solution
Kellogg's solution	0.4 g/mL D-glucose, 5 mg/mL L-glutamine, 0.5 mg/mL Ferric nitrate [$Fe(NO_3)_3$*$9H_2O$], Carboxylase 0.002 % f. c.; Kellogg's solution has to be sterilfiltered with a 0.22 µm filter.
LB media:	10 g/L Tryptone, 5 g/L Yeast extract, 5 g/L NaCl For plates: add 15 g/L agar
LBA media:	LB media with 100 µg/mL ampicillin as selection marker
RAW264.7 media	Adv. DMEM, 10 % FBS, 1x Glutamax
THP-1 media	RPMI 1640 with L-Glutamine, 10 % FBS

Primer sequences for cloning:

Primer name	Sequence (5'→3')	Restriciton enzyme
F51	ACGGTTCAG==GGATCC==GCTACCGATACCG	BamHI

R164	CGTCCC`AAGCTT`TTCTTTCGCAAAATTC	HindIII
F377	TGTCGGC`GGATCC`CTAAACGTCAATCAGC	BamHI
R502	GCGGTTGTT`AAGCTT`TTGCGCCACACC	HindIII
Rev109/124	TCAGCGAGTAGGCTTTGAGGGTAACGGTTG	
For124/109	CCTCAAAGCCTACTCGCTGAAAAAGAGCTG	

Buffers for protein purification:

Denative equilibration buffer	Equilibration/wash buffer with 8 M urea
Denative wash buffers	Equilibration/wash buffer with 7 M to 0 M urea.
Elution buffer	50 mM Na_3PO_4, 300 mM NaCl, 150 mM Imidazole, pH=7
Equilibration/wash buffer	50 mM Na_3PO_4, 300 mM NaCl, pH=7

Buffer for outer membrane preparation:

| Proteinase K 10x Buffer | 500 mM Tris base, 10 mM $CaCl_2$, 20% Glycerol pH=8 |
| TE Buffer | 10 mM Tris-HCl, 1 mM EDTA, pH=8 |

Agarose gel electrophoresis:

10x TAE	48.4 g/L Trizma-base, 3.72 g/L EDTA, 11.42 mL glacial acetic acid
Agarose gel for DNA seperation	1 % agarose in 1x TBE
Agarose gel for RNA seperation	1.2 % agarose in 1x TAE

SDS-PAGE:

5x sample buffer	4 mL H_2O, 1 mL 0.5 M Tris-HCl pH=6.8, 0.8 mL 99 % glycerol, 1,6 mL 10 % SDS (w/v), 0.4 mL β-mercaptoethanol, 0.2 mL 0.05 % bromphenol blue (w/v)
Destaining solution	10 % propanol, 10 % glacial acetic acid
Quick stain solution	35 % 2-propanol, 15 % glacial acetic acid, 0.6 g/L Coomassie Brilliant blue G250

Running buffer   25 mM Tris

192 mM Glycine

0,1 % SDS

pH=8.6

Gel #1: Final volume sufficient for 2 gels:

	12.5 % separation gel	4.5 % stacking gel
H_2O	6.55 mL	6.375 mL
40 % AA/Bis (29/1)	4.7 mL	1.125 mL
1.5 M Tris, pH=8.8, 0.4 % SDS	3.8 mL	--
0.5 M Tris, pH=8.8, 0.4 % SDS	--	2.5 mL
TEMED	20 µL	15 µL
10 % ammonium persulfate	55 µL	40 µL

Gel #2: Final volume sufficient for 2 gels

	10 % separation gel	3 % stacking gel
H_2O	7.5 mL	6.75 mL
40 % AA/Bis (29/1)	3.8 mL	.75 mL
1.5 M Tris, pH=8.8, 0.4 % SDS	3.8 mL	--
0.5 M Tris, pH=8.8, 0.4 % SDS	--	2.5 mL
TEMED	20 µL	15 µL
10 % ammonium persulfate	55 µL	40 µL

2.2 Methods

2.2.1. Bacterial and cell culture

E. coli strains were cultured in LB media or on plates. *N. meningitidis* strains were cultured on GC plates. All bacterial strains were incubated at 37°C and 5 % CO_2. RAW264.7 cells were cultured in the corresponding media (see list) and splitted 1+4 when the cells reached a confluence of around 80 %, i. e. every 3 to 4 days. THP-1 cells were cultured in the corresponding media (see list) and splitted when the cells reached a concentration of around 1000000 cells/mL. The concentration of THP-1 cells should be kept between 200000 and 1000000 cells/mL. All cell lines were propagated in 25 cm^2 or 75 cm^2 T-flask, depending which volume was needed for the experiments.

2.2.2. Production of chemically competent BL21(DE3) *E. coli*

50 mL LB medium was inoculated with BL21(DE3) and incubated at 37 °C until the suspension reached an OD_{600} of 0.2. Bacteria were harvested with centrifuging at 4000 g for 15 min at 4 °C. The supernatant was discarded and the bacterial pellet was suspended in 10 mL of ice cold 30 mM $CaCl_2$ and 10 mM 3-(N-morpholino)propanesulfonic acid (MOPS) at pH=6.8. Immediately after suspending, bacteria were harvested again as mentioned above. The pellet was subsequently suspended in 1.25 mL of ice cold 75 mM $CaCl_2$ and 10 mM MOPS at pH=6.8. The suspension was incubated on ice for 45 minutes and finally 50 µL aliquots were made and stored in the -80 °C freezer.

2.2.3. Cloning of different NhhA fragments and transformation of the vectors into TOP10 *E. coli* and BL21(DE3) *E. coli* respectively

Three different NhhA gene fragments were produced and subsequently cloned into pET21a vectors. The fragments were named *nhhA*-FN for the N-terminal fragment of NhhA from amino acid 51 to 164, *nhhA*-FC for the C-terminal fragment from amino acid 377 to 502 and *nhhA*-FNAss for an assembled fragment stretching from amino acid 51 to 164 but without amino acids 110 to 123 (see figure 5). Genomic DNA from *N. meningitidis* strain FAM20 was used as template. Amplification of the desired PCR product was performed according to the Phusion™ High Fidelity DNA Polymerase kit by Finnzymes. Briefly, approximately 600 ng genomic FAM20 DNA was used as template, buffer, dNTPs, the corresponding primer pair at a final concentration of 10

µM and the Phusion™ polymerase were pipetted together and a PCR was run. This common method results in the desired *nhhA*-FN and *nhhA*-FC fragments with a BamHI and a HindIII restriction site.

Table 1: PCR program used.

	Temperature	Time	Cycles
Initial denaturation	98 °C	30 sec	1
Denaturation	98 °C	10 sec	
Annealing	60 °C	20 sec	34x
Extension	72 °C	20 sec	
Final extension	72 °C	10 min	1
	4 °C	∞	

For *nhhA*-FNAss the common procedure had to be altered. First two PCR products were generated in two separate PCR. For the first fragment primer pairs F51 and Rev109/123 and for the second fragment primer pairs For124/109 and R164 were used. After purification of the amplicons according to the spin protocol with the E.Z.N.A.™ Cycle-Pure Kit the two products were assembled to the *nhhA*-FNAss amplicon. To achieve that, the two fragments were pipetted together in an equimolar manner (310 ng each). Buffer and dNTPs were added according to the Phusion™ High Fidelity DNA Polymerase kit. To finally assemble the fragments, F51 and R164 were used as primer pair and the final concentration was reduced to 0.4 µM. The PCR was run with the aforementioned program.

The following procedure is the same for all fragments. The amplicons needed to be purified (see above) and, like the pET21a vector, separately digested with BamHI and HindIII. The digestion solution contained around 2 µg of an amplicon or 3 µg of pET21a, 2.5 µL of each digestion enzyme, 5 µL of the 10x Fast Digest buffer and the remainder volume to 50 µL was water. After incubation at 37 °C for 2 h all digestions needed to be purified (see above). Additionally, pET21a needed to be dephosphorylated by adding appropriate amounts of FastAP, 10x FastAP buffer and water. For 49 µL of 3 µg purified and digested pET21a vector 4 µL FastAP, 6 µL 10x buffer and 1 µL water was added. Finally the amplicon had to be ligated into pET21a. The weight ratio between vector and amplicon should approximately be 5:1. Ligation is performed in 1x ligation buffer with 10 % of T4 ligase and the appropriate

concentration of amplicon and pET21a vector. This ligation cocktail was incubated at room temperature over night.

After finishing ligation, the vectors containing the inserts *nhhA*-FN and *nhhA*-FC respectively, were transformed into TOP10 *E. coli* bacteria. This was carried out exactly according to the instructions given for the chemical transformation procedure in the manual to the One Shot® TOP10 Competent Cells by Invitrogen™. The only exception was the usage of LB plates containing ampicillin. After incubation over night, small aliquots of 3 mL LBA medium were inoculated with randomly selected colonies. After additional incubation over night, 2 mL of the culture was used to isolate plasmid with the E.Z.N.A.™ Plasmid Miniprep Kit I. 900 μL of the remaining culture were used for a glycerol stock. After isolating the plasmid, it was transformed into BL21(DE3) *E. coli* as follows. 5 μL of plasmid were added to 50 μL of chemically competent BL21(DE3) and incubated on ice for 30 min. A heat shock was subsequently performed at 42 °C for exactly 35 sec. Then another 2 min incubation period on ice follows. After that 700 μL pre-warmed LB medium was added to the bacteria and incubated for 1 h. Finally, the cells were plated onto LB plates containing ampicillin. On the next day, several colonies were randomly picked and 3 mL of LBA medium was inoculated with these. After incubation over night, 2 mL were used to isolate the plasmid and 900 μL were used for a glycerol stock. The plasmid was digested with BamHI and HindIII and analyzed with 1% agarose gel. Additionally, it was sent for sequencing. All following experiments were performed using bacteria from glycerol stocks where the correct insertion and sequence has been verified by sequencing.

For the *nhhA*-FNAss fragment the TOP10 step was skipped. The ligation product was directly transformed into BL21(DE3) bacteria. For procedure see above. This was also confirmed by sequencing.

The strains are in the following termed as BL21(DE3)+NhhA-FN, BL21(DE3)+NhhA-FC and BL21(DE3)+NhhA-FNAss.

2.2.4. Expression and purification of NhhA fragments

10 mL of LBA medium were inoculated with BL21(DE3)+NhhA-FL, BL21(DE3)+NhhA-FN, BL21(DE3)+NhhA-FC or BL21(DE3)+NhhA-FNAss respectively and incubated over night at 37 °C and 160 rpm. 50 mL of LBA medium was inoculated with 2.5 mL of the over night culture. The bacteria were incubated at 37 °C and 160 rpm until the suspension reached an optical density of $OD_{600}=0.6$,

then protein expression was induced by addition of isopropyl β-D-1-thiogalactopyranoside (IPTG) to a final concentration of 1 mM. After 4 h of additional incubation the bacteria were harvested by centrifuging at approx. 4000 g and 4 °C for 15 min. The supernatant was discarded. The bacterial pellet can be stored at -20 °C. 1.5 mL of Talon® resin beads were transferred into a 15 mL tube and pelleted by centrifuging at 700 g for 2 min. The supernatant was discarded and the pelleted beads were washed two times with 15 mL equilibration/wash buffer. Then the pellet was suspended in 5 to 10 mL of the same buffer and transferred to an Econo-Column®. After the beads sedimented the buffer was drained out of the column. The bacterial pellet was suspended in approx. 3 mL of equilibration/wash buffer and subsequently lysed with sonication. The program use was: 5 min. overall sonication time, 30 sec. sonication, 1 min pause, 30 % intensity. The debris was pelleted by centrifuging at approx. 4000 g and 4 °C for 20 min. The supernatant was applied onto the column. 10 µL of supernatant were kept for SDS-PAGE analysis. The protein solution flowed into the resin bed and the flow through was collected. Then, the column was washed twice with five times bed volume of equilibration/wash buffer. This buffer was collected, too. NhhA fragments were eluted by adding five bed volumes of elution buffer. 900 µL were collected of each fraction and 100 µL 99% glycerol was added to enhance stability of the protein fragments. Purity was assessed by SDS-PAGE. For the full-length fragment containing the whole passenger domain without the leader peptide, pure fractions were pooled and concentrated using a centrifugal filter unit.

To purify the protein encoded by *nhhA*-FN the protocol had to be altered. The Talon® resin beads were equilibrated with denative equilibration/wash buffer. The bacterial pellet was suspended and sonicated in this buffer, too. After applying the supernatant onto the column and draining the liquid, the column had to be washed with wash buffers containing decreasing amounts of urea starting with 7 M and finishing after 8 washing steps with 0 M urea. After that, the protein was eluted as described before.

Protein concentration was subsequently measured with a Bradford assay performed according to the Microtiter Plate Protocol in the Protein Assay manual by Bio-Rad. Purified protein fragments are in the following referred to as NhhA-FN for the protein product of *nhhA*-FN, NhhA-FC for *nhhA*-FC and NhhA-FL for the protein containing the whole passenger domain without the leader peptide.

2.2.5. Outer membrane preparation of FAM20

GC plates were inoculated with *N. meningitidis* FAM20 over night. On the next day, several colonies were suspended in 30 µL of sterile distilled water. The protein concentration was determined and the whole cell lysate was diluted to a protein concentration of 0.5 mg/mL. After that, 28 µL of 2% SDS in TE buffer was added to 8 µL of the whole cell lysate. 8 µL proteinase K in 10x proteinase K buffer was added to a final concentration of 3.63 µg/mL. Subsequently, incubation at 60 °C over night follows. For longer storage, the outer membrane preparation was put into the -20 °C freezer.

2.2.6. Apoptosis Assays

2.2.6.1. Apoptosis Assays with recombinant protein

200 µL aliquots of RAW264.7 cells with a density of 10000 cells/mL were seeded in 96 well plates in their growth media supplemented with 1x PeSt. After incubation for 4 h the media was aspirated and 100 µL of fresh media was added. Subsequently the cells were treated with 400 nM NhhA-FL or left untreated as a control. After 21 h of incubation at 37 °C and 5 % CO_2 the media was discarded and a solution of 100 µL growth media supplemented with 1x PeSt and 5 µL of APOpercentage™ dye was pipetted onto the cells. 30 min incubation at growth condition followed. Afterwards the cells were washed with 1x PBS and the apoptotic and viable cells were counted using an Axiovert 40C light microscope with a 400 fold magnification. Of each well three counts were performed starting at the very edge of each well. After the first count, the plate was shifted in order to count the cells next to this first counting window. The third count was performed in the same manner.

200 µL aliquots of THP-1 cells with a density of 50000 cells/mL were seeded in 96 well plates in their growth media supplemented with 1x PeSt. The cells were treated with PMA (c_{stock}=50 µg/mL in DMSO) at a final concentration of 0.1 µg/mL and incubated at their growth conditions for 72 h to induce differentiation to macrophage like cells. A similar protocol was reported by Daigneault et al. (*44*). The media was discarded and 200 µL of fresh growth media with 1x PeSt was added. The cells were subsequently treated with 400 nM NhhA-FL. The following procedure is the same as it was for the RAW264.7 cells.

For both experiments, controls were non-treated cells.

2.2.6.2. Apoptosis Assays with *N. meningitidis strains*

200 µL aliquots of RAW264.7 cells with a density of 20000 cells/mL were seeded in 96 well plates in their growth media. GC plates were inoculated with FAM20 and FAM20ΔnhhA mutant, respectively. After incubation over night approximately 2 mL of DMEM was inoculated with bacteria from the plates. After measuring the OD_{600} of the bacterial solution, cells were subsequently infected at a multiplicity of infection (MOI)=100 with FAM20 and FAM20ΔnhhA strains respectively. After incubation for 21 h at growth conditions 10 µL of APOpercentage™ dye was added to each well. The following procedure is the same as described above.

200 µL aliquots of THP-1 cells with a density of 50000 cells/mL were seeded in 96 well plates in their growth media. The cells were treated with PMA at a final concentration of 0.1 µg/mL and incubated at their growth conditions for 72 h to induce differentiation to macrophage like cells. The media was replaced with a fresh one and cells were infected at a MOI=100 with FAM20 and FAM20ΔnhhA strains respectively. The following procedure is the same as for the RAW264.7 cells.

For both experiments, controls were non-treated cells.

2.2.6.3. Flow cytometry-assisted apoptosis assay with undifferentiated THP-1 cells

Apoptosis measurement by flow cytometry was executed as described before (*45*). 1.5 mL of undifferentiated THP-1 cells with a density of 213000 cells/mL were seeded in 6-well plates. The cells were treated with 400 nM NhhA-FL, 0.5 µg/mL LPS or left untreated respectively. After incubating at growth conditions for 21 h the plates were shaken briefly to suspend pelleted cells and then an aliquot of 500 µL was pipetted into an eppendorf tube. The aliquot was stained with 3.13 µL of APOpercentage™ dye at 37 °C and 5 % CO_2 for 30 min. The cells were harvested by centrifuging at 500 g for 10 min and washed with 500 µL PBS. Finally, the cells were suspended in 500 µL of PBS and filtered into flow cytometer tubes with 30 µm filters by BD. The cells were analyzed using an LSRFortessa™ II from BD with the settings usually used for the PerCP™Cy5.5 dye. Data was analyzed with FACSDiva.

2.2.7. Western blot

To obtain the samples 1 mL of RAW264.7 cells at a density of 100000 cells/mL were seeded into wells of 12-well plates. Then the cells were treated with different NhhA-FL concentration, namely 10 nM, 100 nM and 400 nM in duplicates. One aliquot is

left untreated to serve as the obligatory control. One replicate of each condition was scraped after 6 h of incubation at growth conditions. The resulting cell suspension was pipetted into an eppendorf tube and stored at -20 °C. The other replicates were collected after 21 h. Subsequently 50 µL of each sample were transferred into a new eppendorf tube and washed twice with 50 µL PBS. To pellet the cells 500 g for 5 min were applied. Finally, the cells were suspended in 10 µL of PBS, an appropriate amount of 5x SDS sample buffer was added and the samples were heated at 95 °C for 5 min. Then an SDS-page was run with gel #1. The PVDF+ membrane was cut out in the correct size and put into methanol for 30 sec, then into water for 5 min and subsequently into transfer buffer for 10 min. Two whatman papers were soaked with transfer buffer and the SDS-gel was also put into it for approximately 3 min. The parts were assembled as shown.
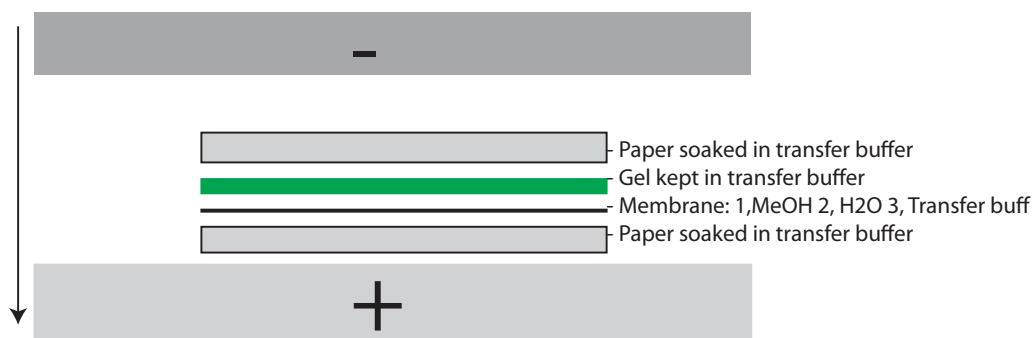
Fig. 7: Scheme of how all parts should be assembled for western blotting.

Then the protein was transferred to the membrane by running the blot for 15 minutes at 15 V. The membrane was rinsed with PBS and subsequently blocked with 5 % skim milk dissolved in PBS for 1 h at room temperature. The 1st antibody (mouse IgG anti NhhA) was diluted 1:500 times with 0.1 % Tween-20 in PBS and added to the membrane. Dr. Jafar Mahdavi recommended this dilution. Incubation at 4 °C over night follows. On the next day, the membrane was washed three times with 0.1 % Tween-20 in PBS for 10 min each. The 2nd antibody (680-donkey anti mouse) was diluted 1:15000 times with 0.1 % Tween-20 in PBS and added to the membrane. After incubation for 1 h at room temperature the membrane was washed as indicated before. Before scanning, the membrane had to be rinsed with PBS.

2.2.8. siRNA transfection

RAW264.7 cells were transfected with two siRNAs against TLR1, TLR2, CD14 and MyD88 each and a control siRNA as described in the manual of Qiagens transfection agent. In brief, 20000 cells in 30 µL of growth medium were seeded per well of a 96-

well plate. siRNAs were diluted with 30 µL growth medium without serum to a f. c. of 50 nM, then 1 µL transfection reagent was added and mixed. After 10 min of incubation this solution was added slowly to the cells. Additional 6 h of incubation at growth conditions followed before 140 µL complete growth medium was added. All further experiments with siRNA-transfected cells were started after over night incubation.

Knockdown efficiency was either assessed with RT-qPCR analysis or with 21 h treatment of Pam3CSK4 (f. c. is 50 ng/mL), a TLR1/2 agonist, or LPS (f. c. is 0.5 µg/mL), a TLR4 agonist, respectively.

2.2.9. ELISA

ELISA assays were performed exactly according to the manual of the corresponding kits. Non-transfected or RAW264.7 cells transfected with siRNAs TLR1_1, TLR2_2, CD14_1, MyD88_4, AllStar n. c. siRNA were treated with 400 nM NhhA-FL for 21 h. Media were collected and Il6 and TNFα concentration was measured. Raw data was analyzed as indicated in the corresponding manual. A 4-parameter curve fit was used to calculate TNFα and Il6 results were obtained from invitrogens ELISA kits. To calculate the results of the Il6 ELI-PAIR kit, a linear regression was used, as pointed out in the manual for this kit.

Controls were cells, which were not treated with NhhA-FL.

2.2.10. RAW264.7 and THP-1 treatment for gene expression assessment

1.5 mL aliquots of RAW264.7 cells with a calculated density of c=666666 cells/mL were seeded into 6-well plates. This results in a density of 1000000 cells/well. The cells were incubated at growth conditions over night. Afterwards the cells were treated with 400 nM NhhA-FL and incubated for 6 h at their growth conditions. The supernatant was discarded and the RNA was isolated (see 2.2.13. qPCR).

1.5 mL aliquots THP-1 cells with a density of c=500000 cells/mL were seeded into 6-well plates. PMA dissolved in DMSO (c_{stock}=50 mg/mL) was added to reach a f. c. of 0.1 µg/mL to induce differentiation. Incubation at growth conditions for 72 h followed. The supernatant was discarded and fresh medium containing 1x PeSt was added to the cells. Then cells were treated for 6 h with 400 nM NhhA-FL or left untreated as a control, respectively.

To investigate the other fragments and the outer membrane preparation, the procedure was the same as mentioned above for the THP-1 cells with the sole

difference that the density of THP-1 cells seeded was only 275000 cells/mL. After differentiation the cells were either treated with 400 nM NhhA-FN, 400 nM NhhA-FC, 400 nM NhhA-FNAss, the outer membrane preparation of FAM20 or left untreated as a control, respectively. For the treatment with the outer membrane preparation three different concentrations were used. The calculated f. c.s were 146 ng/mL, 14.6 ng/mL and 1.46 ng/mL.

To investigate the role of TLR4 in differentiated THP-1 cells, 1.5 mL aliquots of THP-1 cells with a density of c=500000 cells/mL were seeded into 6-well plates and differentiated as mentioned before. The supernatant was discarded and fresh medium containing 1x PeSt was added to the cells. CLI-095, a TLR4 antagonist, was added to reach a f. c. of 1 µM. After incubation for 1 h at growth conditions NhhA-FL with a f. c. of 400 nM was added and an additional incubation at the aforementioned conditions for 6 h followed.

Again untreated cells were used as controls.

2.2.11. Isolation of RNA and cDNA synthesis

RNA had to be isolated with RNeasy® Mini Kit by Qiagen. RNA was isolated either from RAW264.7 or from THP-1 cells treated as indicated in section 2.2.10. or 2.2.8 without treatment of Pam3CSK4 or LPS. RNA quality was assessed by 1.2 % agarose in TAE gel electrophoresis with TAE buffer to check RNA integrity and by nanodrop measurement to determine the concentration and pureness. To run the electrophoresis, agarose was dissolved in TAE buffer by heating to reach a f. c. of 1.2 % (w/v). Then the gel was poured into a rack and after solidifying, TAE buffer was added, the samples were applied and the gel was run with 120 V (*46*).

After verification of the good quality of the RNA, a 1st strand cDNA synthesis was performed. Therefore, Fermentas' RevertAid™ H Minus First Strand cDNA Synthesis Kit was used. For knockdown efficiency measurements, 100 ng RNA was used as template. For all the other experiments 300 ng RNA was used. The oligo(dT)$_{18}$ primer provided by the kit was used for all RT-PCRs. In the end, a final volume of 20 µL cDNA solution was reached. For experiments, where more than 20 µL cDNA was needed, the template amount was doubled and additional 20 µL of water (provided by the kit) was added in order to reach a final volume of 40 µL.

For generating cDNA for the qPCR Array a different synthesis kit was used. The manual RT² Profiler™ PCR Array System by SABiosciences™ recommends the RT²

First Strand Kit. The exact procedure is indicated in the manual. Again 300 ng template RNA was used.

2.2.12. qPCR array

The Toll-Like Receptor Signaling Pathway PCR Array was purchased from SABiosciences™. cDNA synthesized with the kit specifically purchased for the array was used (see above) and additionally a specific SYBR green dye for the LightCycler®, namely the RT^2 SYBR Green qPCR Master Mix, indicated in the manual of the array (see above) was used to ensure best results. Additionally, a different program needed to be run as indicated in the instrument setup instructions for the Roche LightCycler® 480 by SABiosciences™:

Table 2: qPCR program for the array

Heat activation: 1 cycle, analysis mode: none			
Target (°C)	Acquisition Mode	Hold (hh:mm:ss)	Ramp Rate (°C/s)
95	None	00:10:00	4.4
PCR cycle: 45 cycles, analysis mode: quantification			
95	None	00:00:15	1.0
60	Single	00:01:00	1.0
Melt curve: 1 cycle, analysis mode: melting curves			
Target (°C)	Acquisition Mode	Hold (hh:mm:ss)	Ramp Rate (°C/s)	Acquisition (per °C)
60	None	00:00:15	4.4	
95	Continuous		0.03	20

2.2.13. qPCR

For cDNA derived from RNA from RAW264.7 cells, GAPDH was used as reference gene in contrast to samples derived from differentiated THP-1 cells where RPL37A was used as reference gene since GAPDH is not equally expressed in differentiated and undifferentiated THP-1 cells (*47*). The reaction mixtures were composed as indicated in the manuals of the SYBR green dyes. 2 µL of unpurified cDNA solution was used as template. To assess the primer efficiency of the ones used for measuring cytokines, serial dilutions of the cDNA template were performed. cDNA derived from untreated samples were amplified pure, 1:2, 1:4 and 1:8 diluted whereas cDNA derived from NhhA-FL treated samples were amplified pure, 1:10, 1:100 and 1:1000 diluted. The c_p values were plotted against the $\log_{10}$ of the dilution factors in a reversed manner. That means for instance that the c_p value obtained

from a 1:8 (for untreated cells) or a 1:1000 (for NhhA-FL treated cells) diluted sample, respectively, was plotted against $\log_{10}(1)$ on the x-axis. c_p values obtained from pure samples were plotted against $\log_{10}(8)$ for untreated and $\log_{10}(1000)$ for NhhA-FL treated samples. Subsequently, the slopes k were calculated. To finally calculate the efficiency of the primers, the following formula was used.

$$E = \frac{10^{\frac{-1}{k_{untreated}}} + 10^{\frac{-1}{k_{NhhA-FL\ treated}}}}{2}$$

Formula 1: E: efficiency; $k_{untreated}$: calculated slope of the untreated samples; $k_{NhhA-FL\ treated}$: calculated slope of the NhhA-FL treated samples. Modified from the LightCycler® 480 Instrument Operator's Manual.

For primer sequences and efficiencies see the appendix.

Table 3: qPCR program for assessing the knockdown efficiency

Pre-incubation: 1 cycle, analysis mode: none			
Target (°C)	Acquisition Mode	Hold (hh:mm:ss)	Ramp Rate (°C/s)
95	None	00:10:00	4.4
Amplification: 45 cycles, analysis mode: quantification			
95	None	00:00:10	4.4
60	None	00:00:15	2.2
72	Single	00:00:20	4.4

Melting curve: 1 cycle, analysis mode: melting curves				
Target (°C)	Acquisition Mode	Hold (hh:mm:ss)	Ramp Rate (°C/s)	Acquisition (per °C)
95	None	00:00:05	4.4	
65	None	00:01:00	2.2	
97	Continuous		0.11	5

Cooling: 1 cycle, analysis mode: none			
Target (°C)	Acquisition Mode	Hold (hh:mm:ss)	Ramp Rate (°C)
40	None	00:00:10	1.5

Table 4: qPCR program for verification experiments of the cytokine screen

Pre-incubation: 1 cycle, analysis mode: none			
Target (°C)	Acquisition Mode	Hold (hh:mm:ss)	Ramp Rate (°C/s)
95	None	00:10:00	4.4
Amplification: 40 cycles, analysis mode: quantification			
95	None	00:00:15	4.4

60	None	00:00:30	2.2	
72	Single	00:00:30	4.4	
Melting curve: 1 cycle, analysis mode: melting curves				
Target (°C)	Acquisition Mode	Hold (hh:mm:ss)	Ramp Rate (°C/s)	Acquisition (per °C)
95	None	00:00:05	4.4	
65	None	00:01:00	2.2	
97	Continuous		0.11	5
Cooling: 1 cycle, analysis mode: none				
Target (°C)	Acquisition Mode	Hold (hh:mm:ss)	Ramp Rate (°C)	
40	None	00:00:10	1.5	

2.2.14. Data and statistical analysis

Data and statistical analysis was performed by Excel 2003 or Excel 2011. 4-parameter fit curves for ELISA data were obtained by GraphPad Prism®. Student t-tests are always two tailed, homoscedastic tests.

3. Results and Discussion

3.1. Expression and purification of NhhA fragments

Images 8 to 11 show SDS-pages from representative protein purifications.
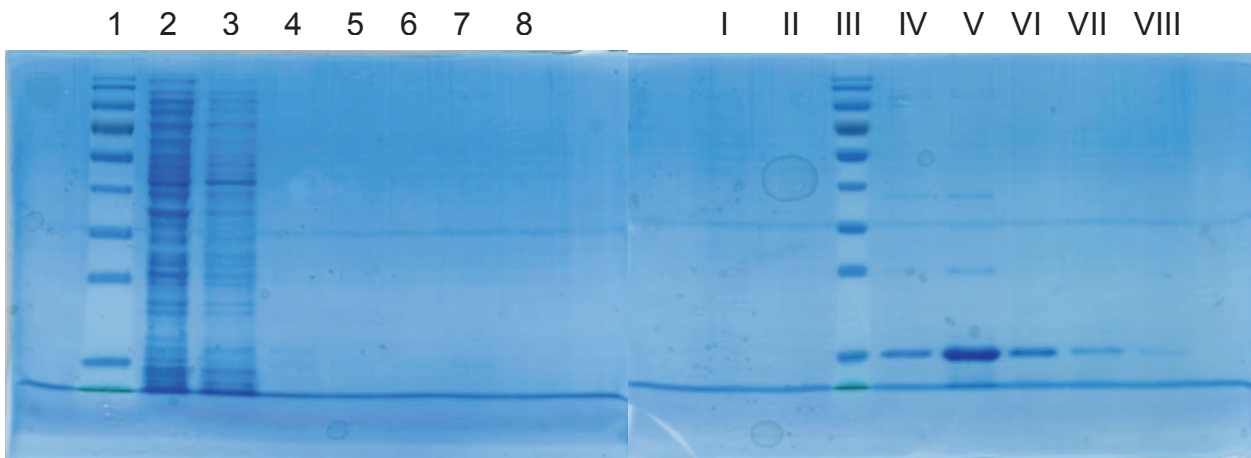
Fig. 8: Purification of NhhA-FN; 1: marker; 2: FT; 3: W1, 7M urea; 4: W2, 6 M urea; 5: W3, 5 M urea; 6: W4, 4 M urea; 7: W5, 3 M urea; 8: W6, 2 M urea; I: W7, 1 M urea; II: W8, 0 M urea; III: marker; IV: E1; V: E2; VI: E3; VII: E4; VIII: E5
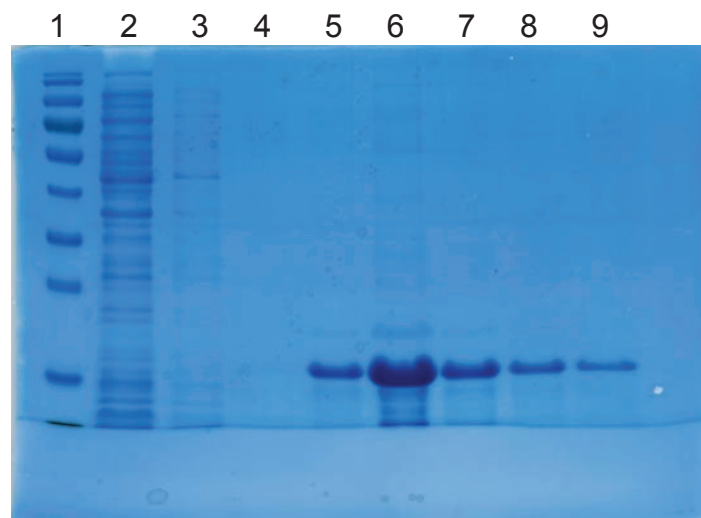
Fig. 9: Purification of NhhA-FC; 1: marker; 2: FT; 3: W1; 4: W2; 5: E1; 6: E2; 7: E3; 8: E4; 9: E5
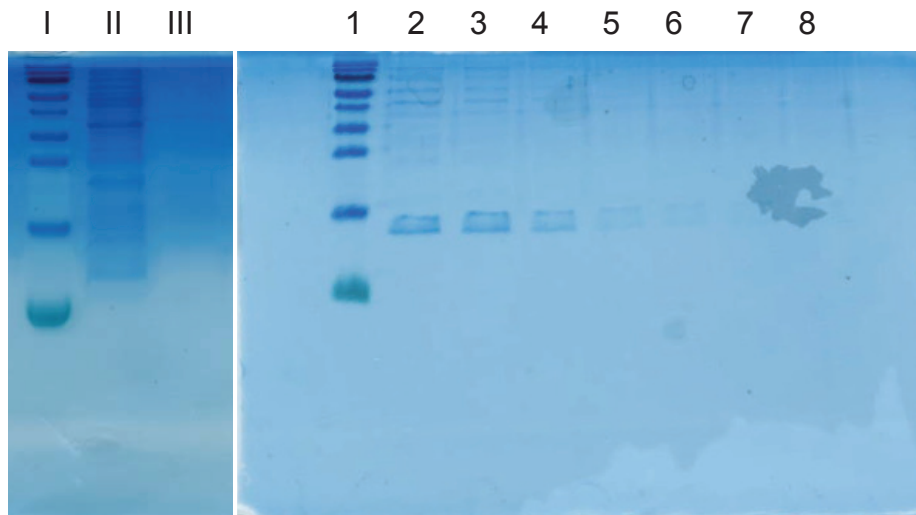
Fig. 10: Purification of NhhA-FNAss; I, 1: marker; II: FT; III: W; 2: E1; 3: E2; 4: E3; 5: E4; 6: E5; 7: E6; 8: E7
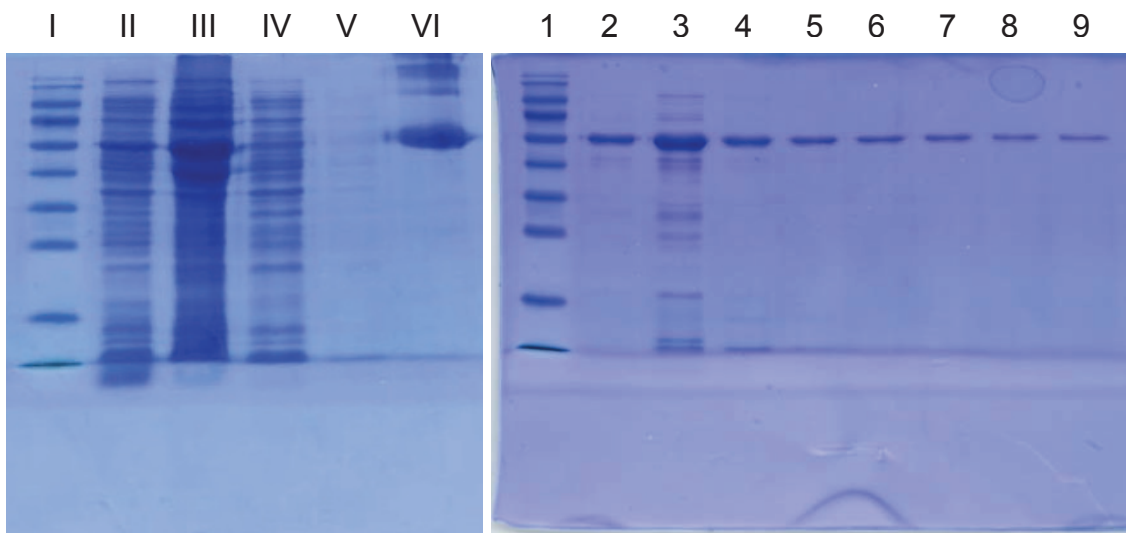
Fig. 11: Purification of NhhA-FL; I, 1: marker; II: non induced lysate; III: induced lysate; IV: FT; V: W1; VI: W2; 2: E1; 3: E2; 4: E3; 5: E4; 6: E5; 7: E6; 8: E7; 9: E9

In order to calculate the concentration, a standard curve was generated by known amounts of BSA. One of these standard curves is shown in fig. 12. With the slope and the y-axis intercept obtained from the regression curves, it was possible to calculate the concentrations of the protein fragments.
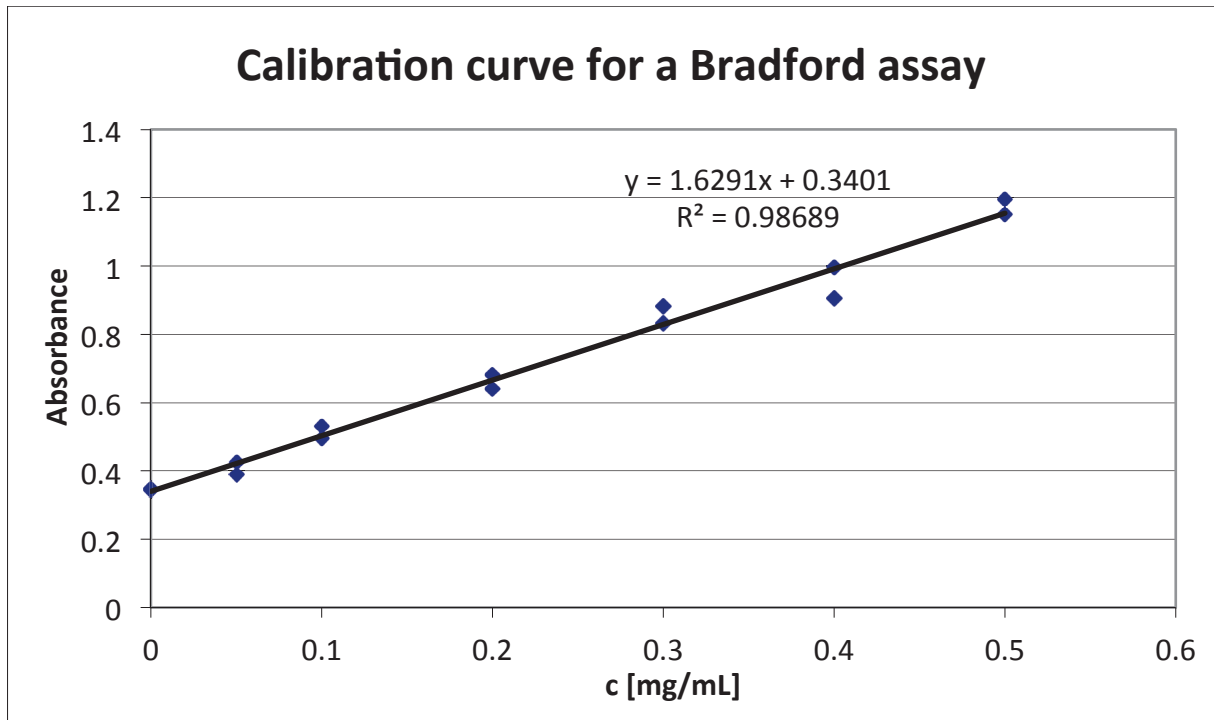
Fig. 12: Representative calibration curve for a Bradford assay to determine protein concentrations.

3.2. Apoptosis Assays

Firstly, it was to be assessed whether the recombinant expressed NhhA-FL induces apoptosis in macrophages. As mentioned before, RAW264.7 and differentiated THP-1 cells were used for these experiments. In the figures 13 and 14 it is shown that this protein fragment significantly induces apoptosis. RAW264.7 cells are macrophage like mouse cells and THP-1 cells are monocytic like human cells, which can be differentiated to macrophage like cells.
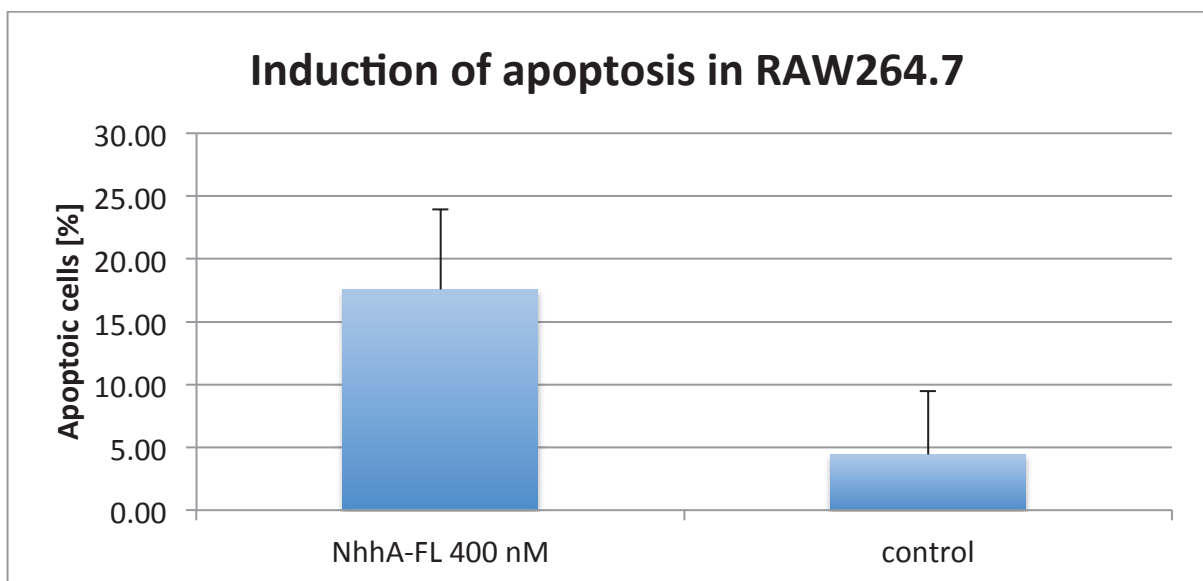
Fig. 13: NhhA-FL induced apoptosis in RAW264.7 cells. The mean and standard deviation of at least six independent replicates is shown. p<0.005
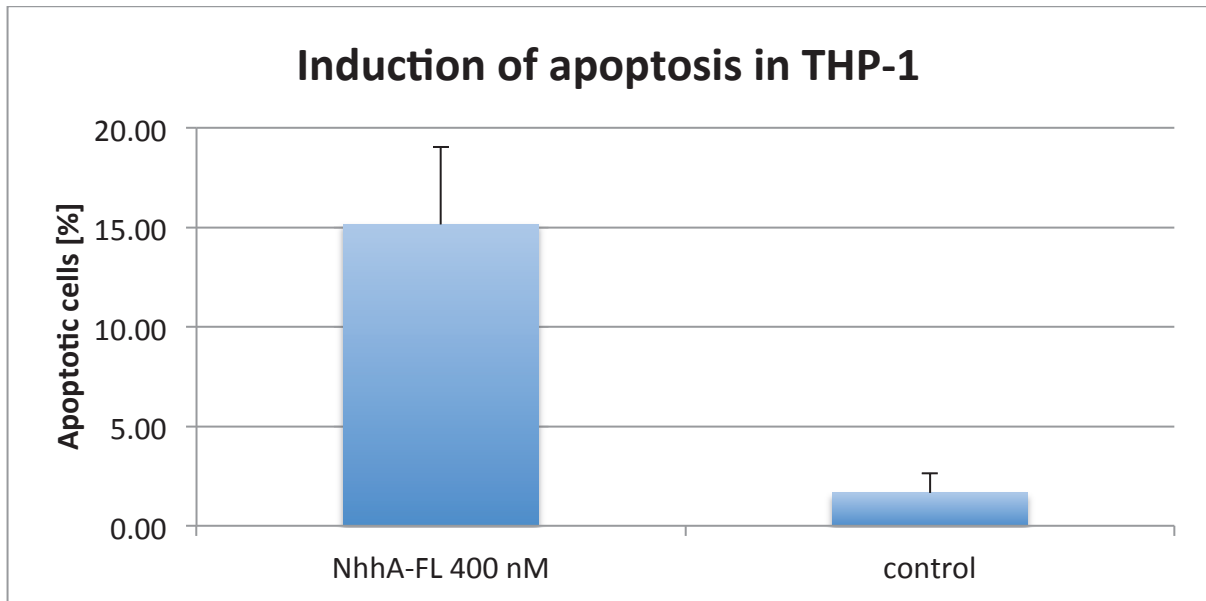
Fig. 14: NhhA-FL induced apoptosis in to macrophages differentiated THP-1 cells. The mean and standard deviation of three independent replicates is shown. p<0.005

To confirm that endogenous NhhA controls apoptosis, induction of apoptosis with FAM20 and FAM20ΔnhhA in RAW264.7 and THP-1 cells was assessed.
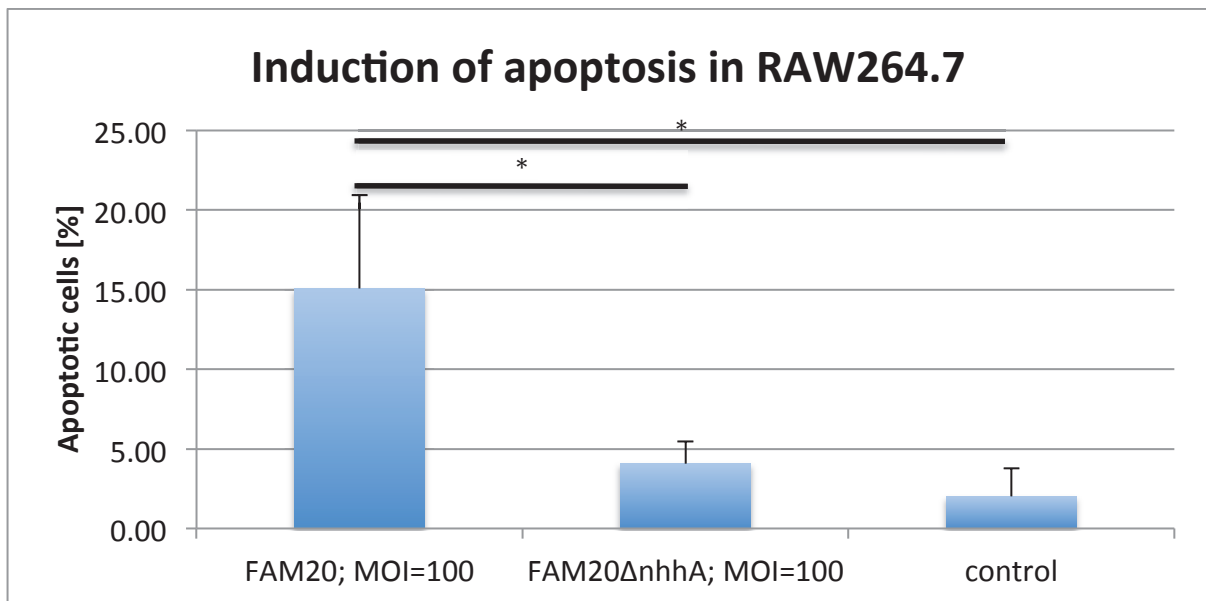
Fig. 15: FAM20 and FAM20ΔnhhA induced apoptosis in RAW264.7 cells. The mean and standard deviation of three independent replicates is shown. *p<0.05
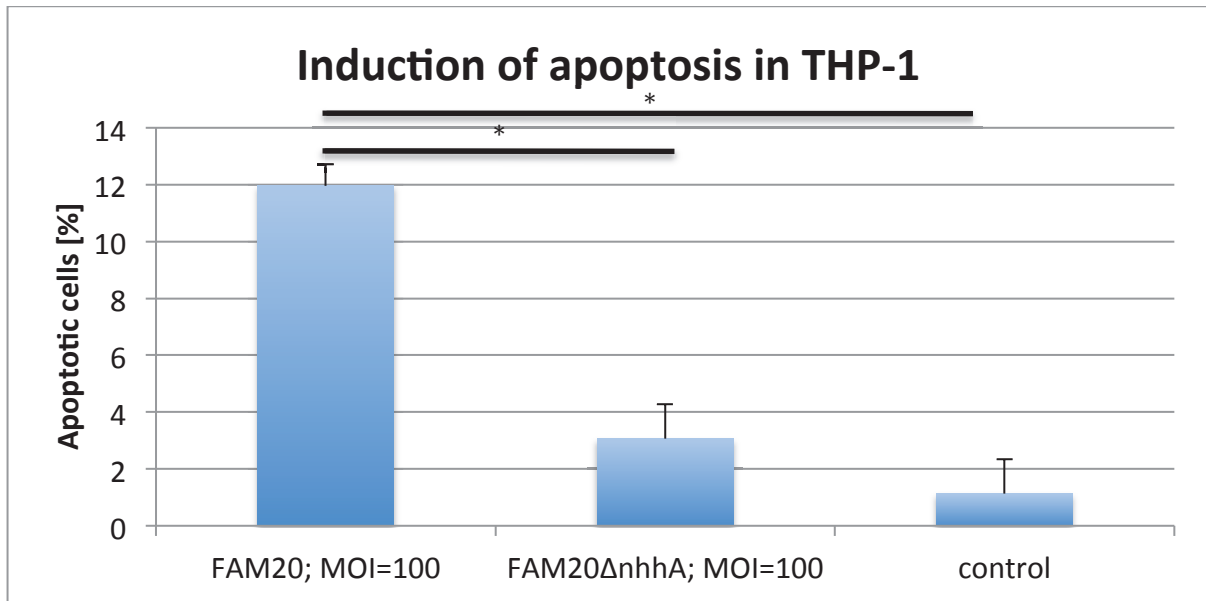
Fig. 16: FAM20 and FAM20nhhA induced apoptosis in differentiated THP-1 cells. The mean and standard deviation of three independent replicates is shown. *p<0.0005

The data presented in figures 17 to 19 is obtained from apoptosis assays done with flow cytometry in order to achieve more robust data from larger cell populations.
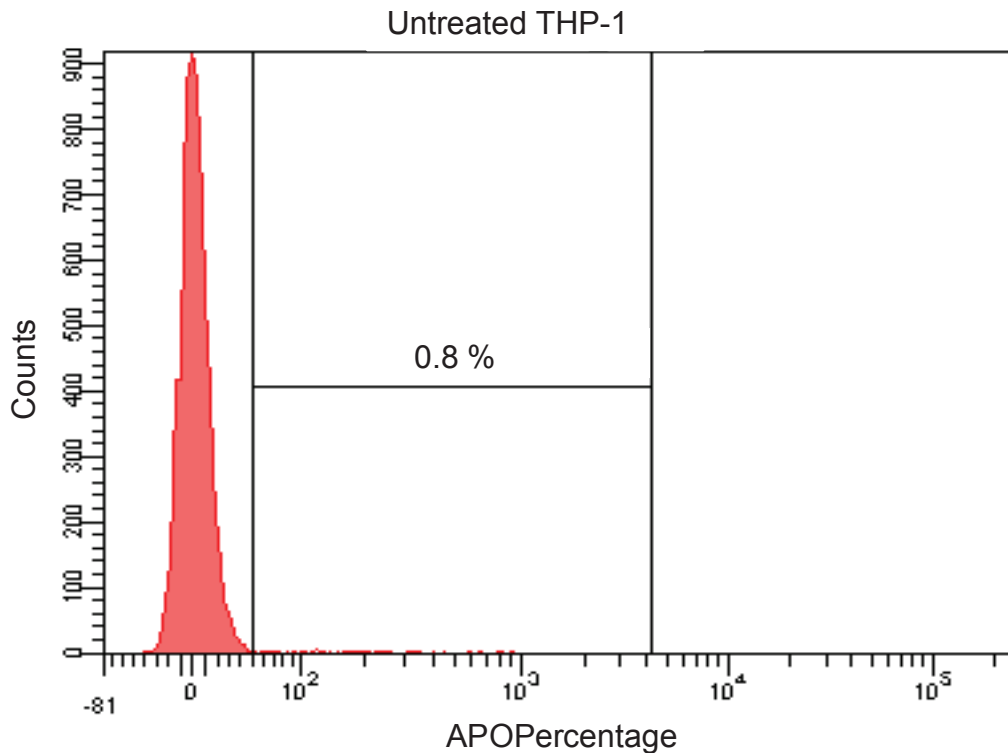
Fig. 17: Untreated THP-1 cells stained with the APOPercentage dye. 0.8 % of the cells are apoptotic.
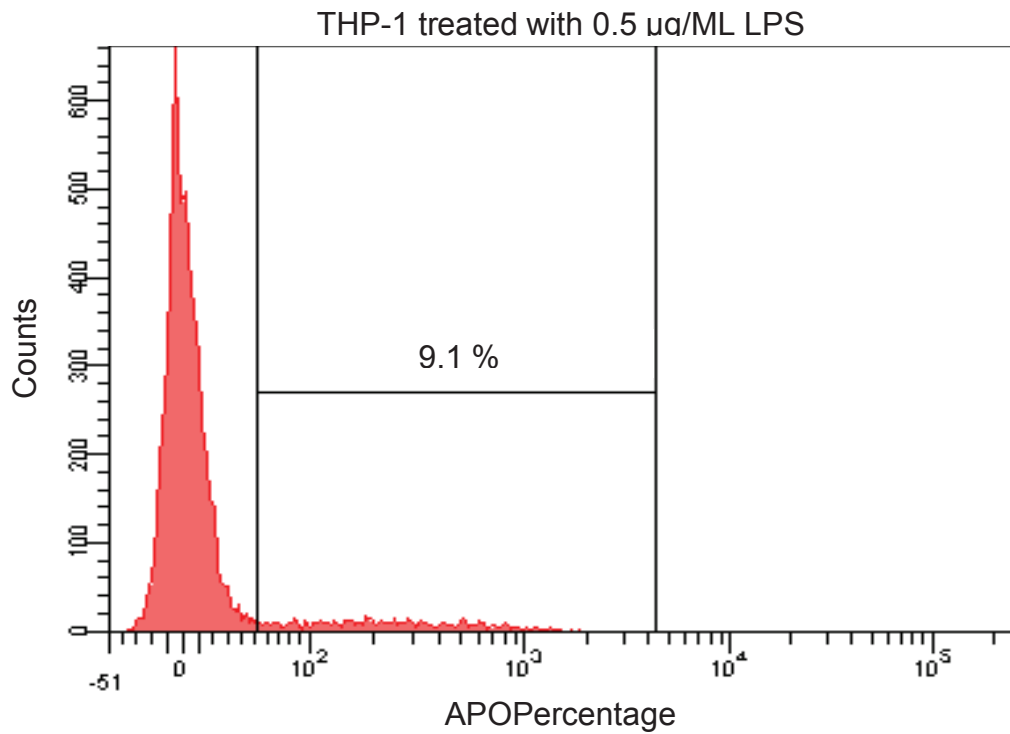
Fig. 18: THP-1 cells treated with 0.5 µg/mL LPS for 21 h and stained with the APOPercentage dye. 9.1 % of the cells are apoptotic.
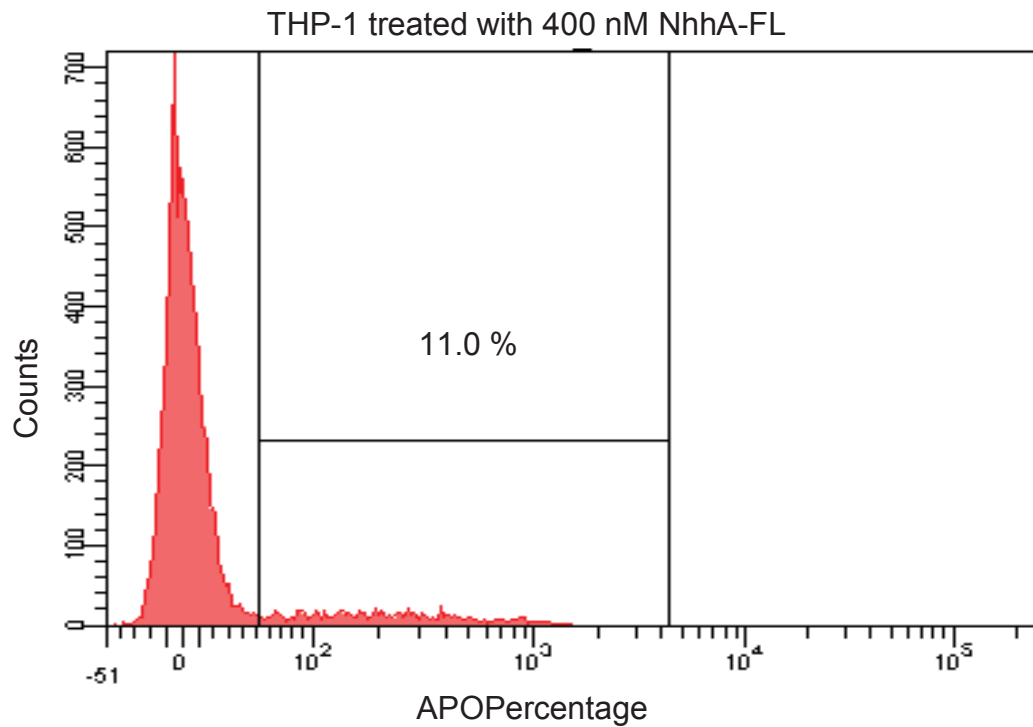
Fig. 19: THP-1 cells treated with 400 nM NhhA-FL for 21 h and stained with the APOPercentage dye. 11.0 % of the cells are apoptotic.

When interpreting these apoptosis experiments one needs to keep in mind that NhhA serves as an adhesion protein (*36*). Therefore, it is unclear whether the reduced induction of apoptosis by the deficient strain is due to reduced binding of bacteria to cells or due to the lacking of the inducer. Despite the remarkable similar results of the experiments where cells were treated with NhhA-FL, this needs to be further investigated. The FACS data obtained from undifferentiated THP-1 cells indicates two things: Firstly, NhhA-FL also induces apoptosis in monocytes and secondly, it shows that the data obtained from the apoptosis assays via counting seems to be true. Errors in the counting procedure might have a severe effect on the results with adherent cells. The results obtained by flow cytometry, however, show that the results achieved by simple counting of apoptotic cells are reliable. Another point of criticism might result in the fact that the ratio of NhhA-FL molecules per cell seems to be very high. For the experiment with RAW264.7 cells, approximately 12E18 molecules NhhA-FL per cell and for the experiments with differentiated THP-1 cells approximately 48E16 molecules NhhA-FL per cell are used. Nevertheless, since cells infected with FAM20 or *nhhA*-FL deficient mutant at a MOI=100 show similar results, 400 nM NhhA-FL treatment is still reasonable.

The overall conclusion of these experiments is that NhhA has severe effects on the viability of macrophages and monocytes, no matter whether these effects come directly from NhhA or are affiliated to the higher binding of bacteria expressing NhhA.

3.3. Il6 and TNFα release

Preliminary data has shown that NhhA-FL induces Il6 and TNFα release (unpublished data). We were able to repeat these experiments and measure cytokine release via ELISA.
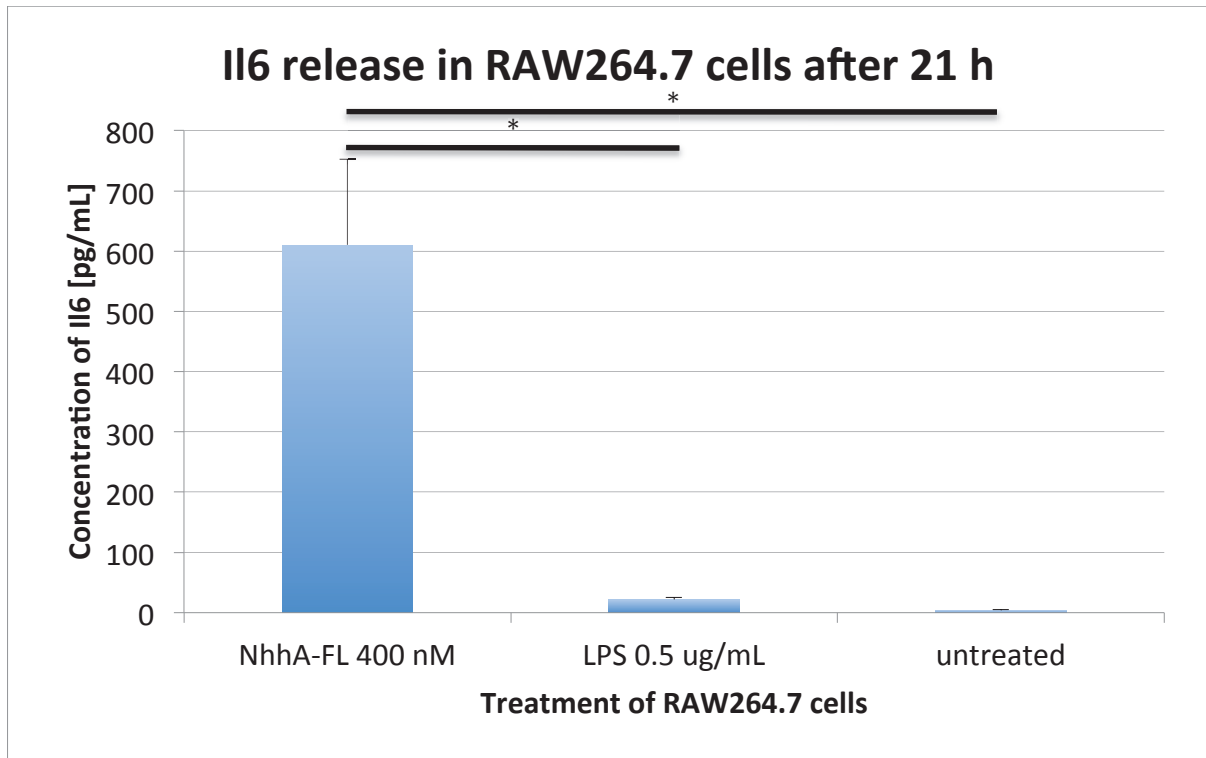
Fig. 20: Il6 release in NhhA-FL treated RAW264.7 cells. Cells were seeded at a density of 20000 cells/mL. The mean and standard deviation of three independent replicates is shown. *p<0.005
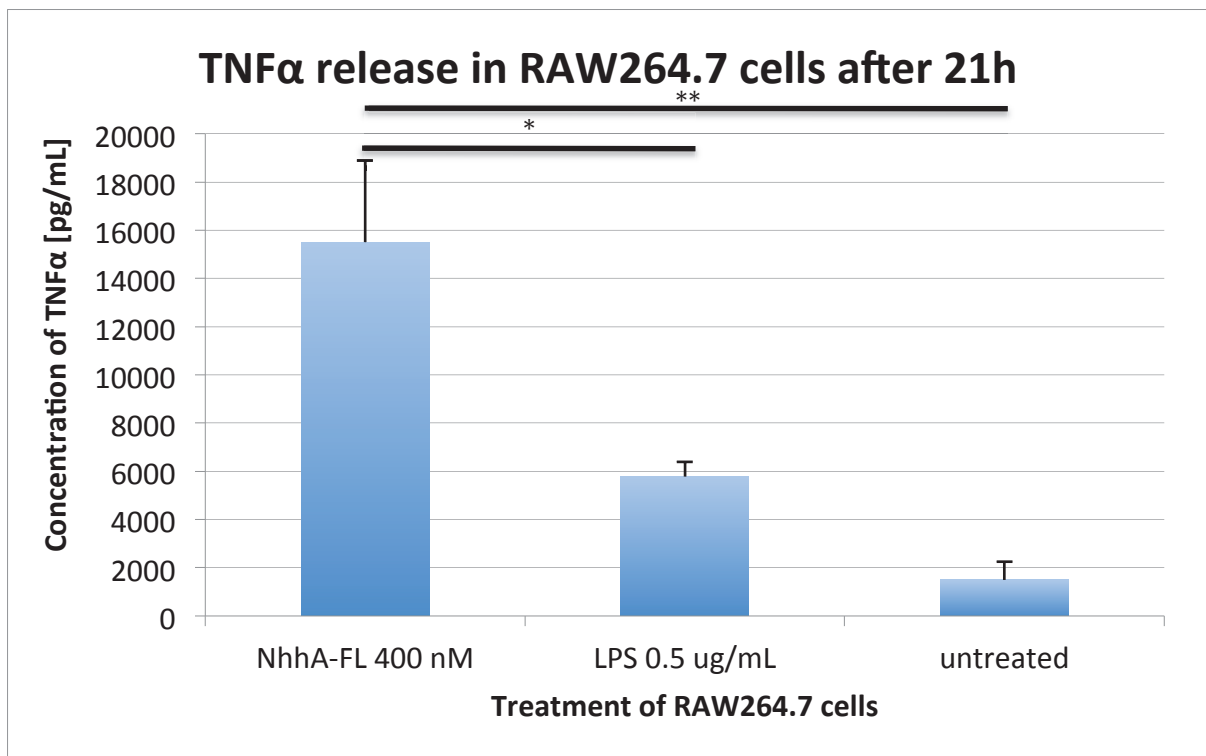
Fig. 21: TNFα release in NhhA-FL treated RAW264.7 cells. Cells were seeded at a density of 20000 cells/mL. The mean and standard deviation of three independent replicates is shown. *p<0.01; **p<0.005

To assess the dose dependence of Il6 and TNFα release, RAW264.7 cells were treated with decreasing concentrations of NhhA-FL starting with 400 nM. The results

indicate a positive correlation between NhhA-FL concentration and Il6 and TNFα release respectively. This indicates that stimulation of cells with 400 nM NhhA-FL or even higher might be required for maximal response.
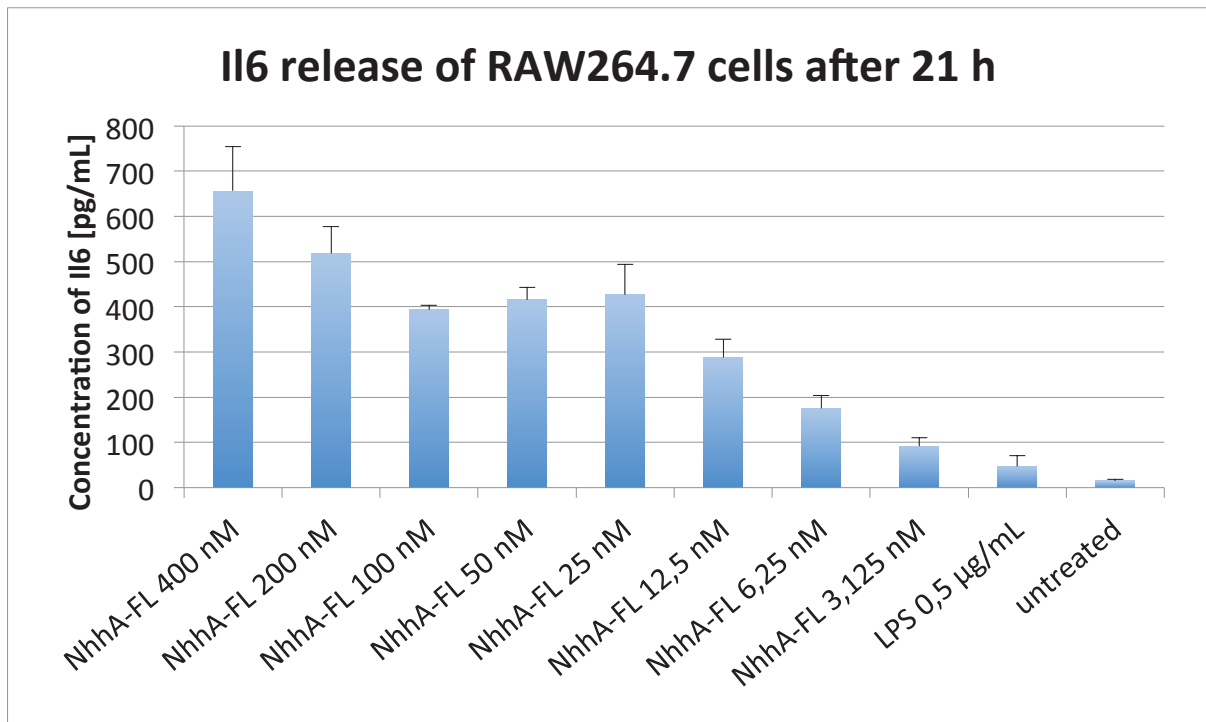
Fig. 22: Dose dependent IL-6 release of RAW264.7 cells after NhhA-FL treatment. The mean and standard deviation of three independent replicates is shown.
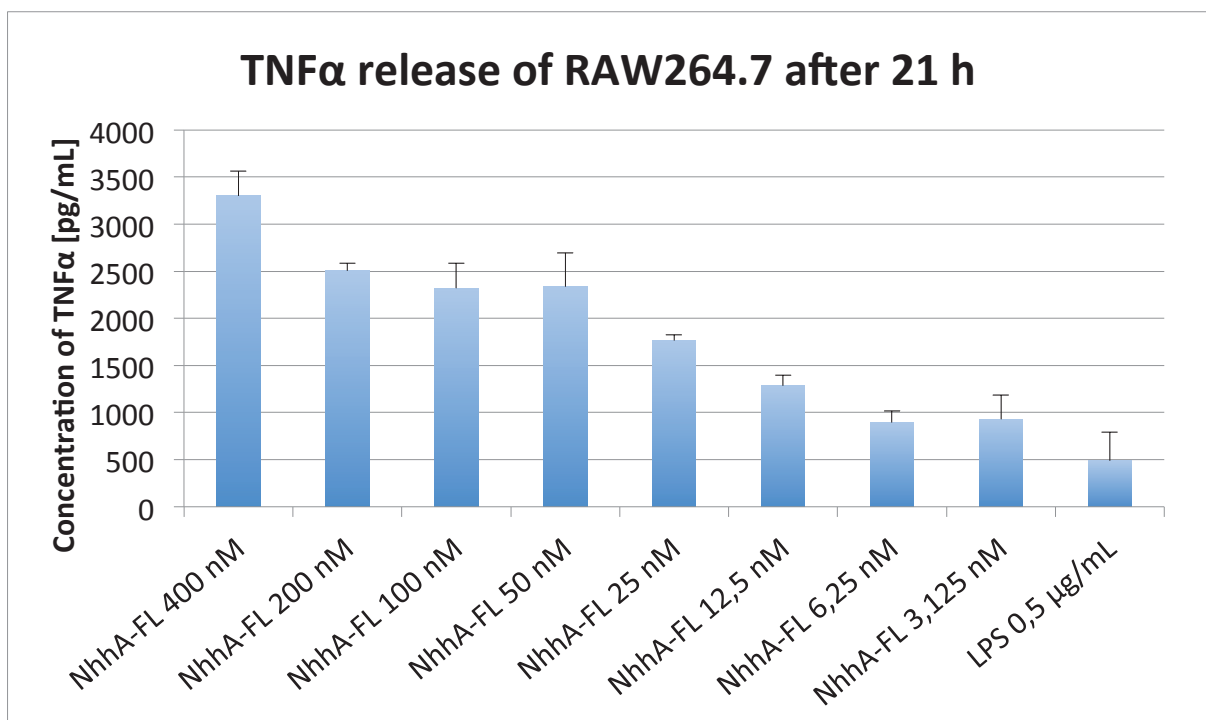
Fig. 23: Dose dependent TNFα release of RAW264.7 cells after NhhA-FL treatment. TNFα release for untreated cells was below the detection limit. The mean and standard deviation of three independent replicates is shown.

The Toll-like receptor (TLR)-signaling pathway is critical for immune response. Overall, ten active TLRs (TLR1 to TLR10) exist in humans and exhibit important functions in gene regulation, particularly in the regulation of expression of proinflammatory cytokines. Detailed reviews are given elsewhere (*48-50*). Preliminary data (not shown) suggested that NhhA-FL at least partly signals via TLR4. By inhibiting TLR4 in RAW264.7 cells with an antagonist (CLI-095) Il6 but not TNFα release was abolished. TLR4 and TLR2 are receptors important for recognition of various cell wall components. Particularly LPS binds to TLR4, but signaling requires the presence of adapter proteins, one of those is CD14. Additionally, TLR4 signaling is either MyD88 dependent or independent (*48-50*). The last step of this signaling cascade is NFκB because inhibition abolished Il6 and TNFα release (data not shown). Therefore, siRNA knockdown against TLR1, TLR2, CD14 and MyD88 was performed and subsequently, NhhA-FL induced Il6 and TNFα release was measured. siRNA knockdown efficiency was assessed with qPCR and treatment of cells with specific agonists of the silenced receptors or adapter protein, namely Pam3CSK4 as agonist for TLR1, TLR2 and MyD88 and LPS as agonist for CD14 and MyD88.
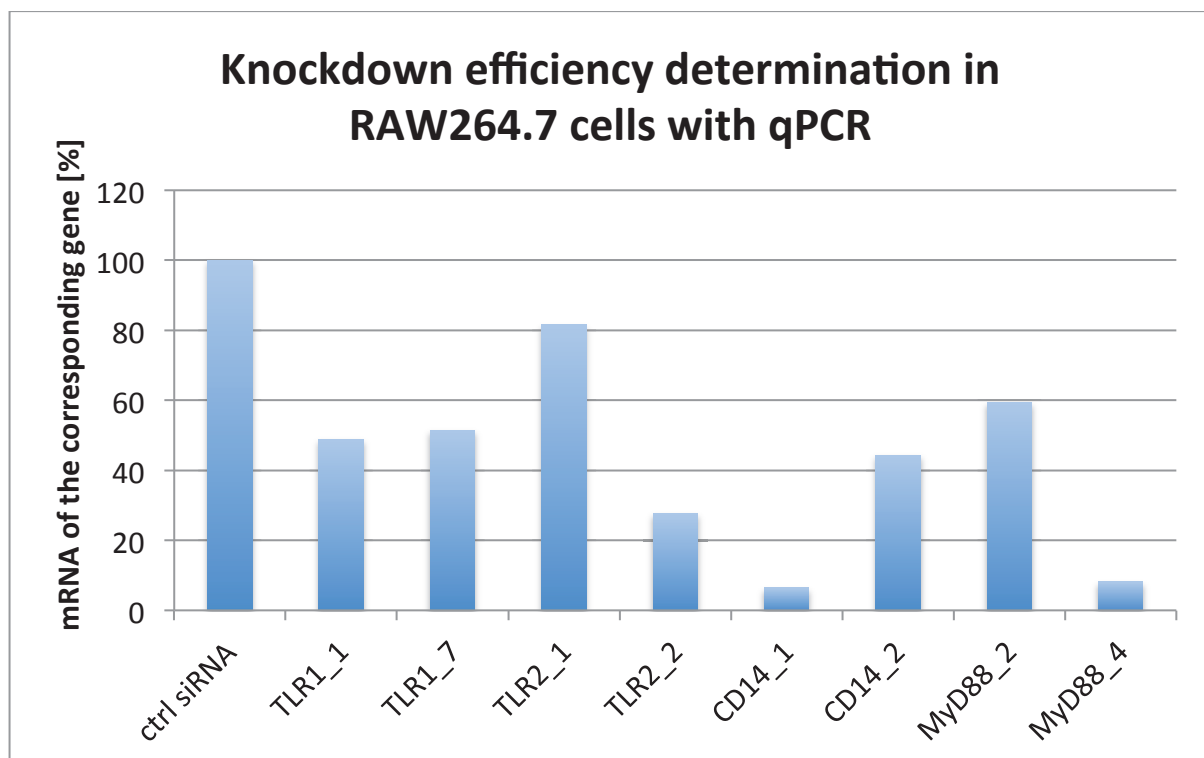
Fig. 24: Knockdown efficiency of siRNAs. The mRNA level targeted by the siRNA was measured for each siRNA treatment individually. For primer sequences see appendix. No RNA integrity was assessed.

Since the siRNAs TLR1_1, TLR2_2, CD14_1 and MyD88_4 are the most potent ones, these were used for further experiments. To determine whether knocking down

of mRNA levels affects protein levels, RAW264.7 cells transfected with siRNAs were treated with Pam3CSK4 and LPS respectively. Results indicated that knocking down of mRNA also affected the protein levels in these experiments.
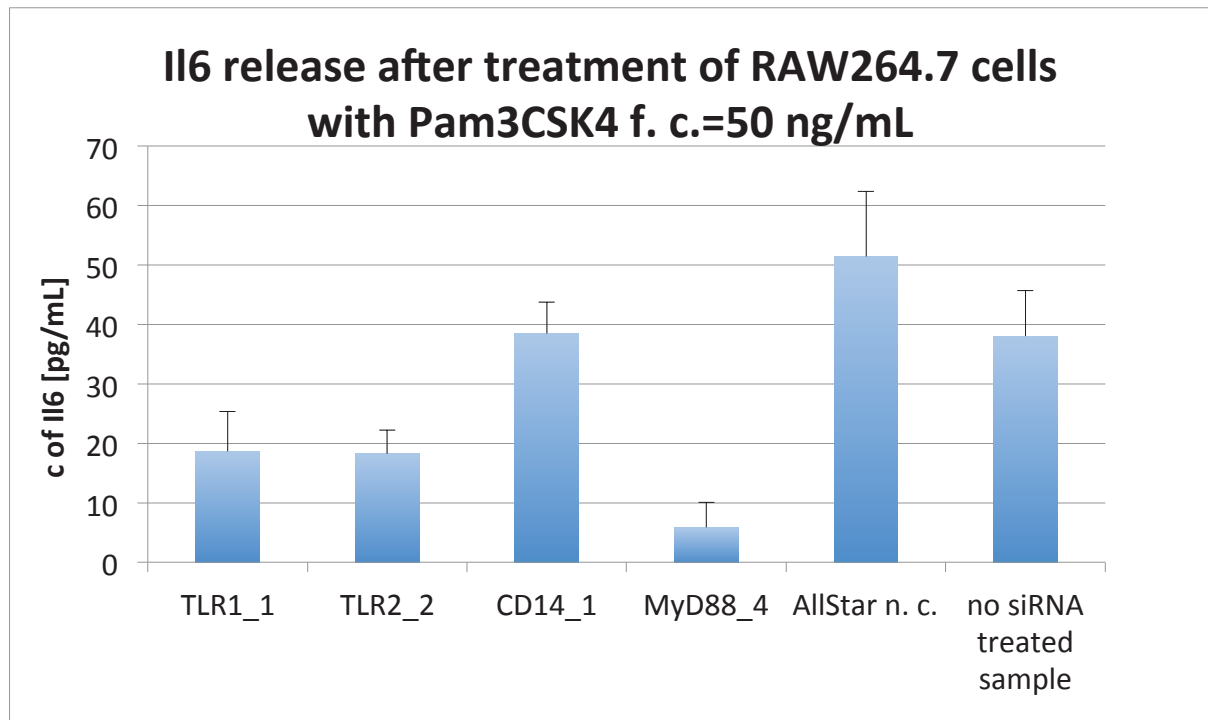
Fig. 25: Il6 release in siRNA treated cells after treatment with Pam3CSK4. The mean and standard deviation of three independent replicates is shown.
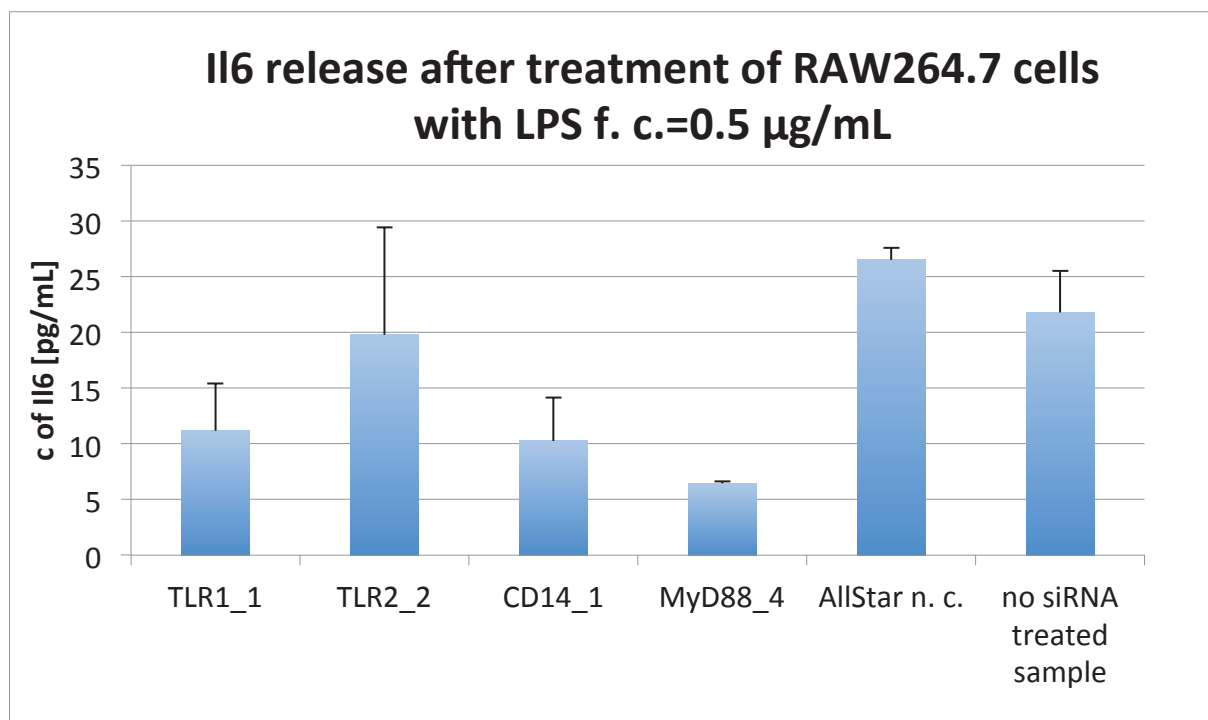
Fig. 26: Il6 release in siRNA treated cells after treatment with LPS. The mean and standard deviation of three independent replicates is shown.

As it is shown in the two figures above, knockdown with TLR1_7, TLR2_2 and MyD88_4 also affects protein levels, as Pam3CSK4 treatment did not induce as high levels of Il6 as treatment of controls. The same refers to LPS and cells treated with siRNAs against CD14 and MyD88. To our surprise the siRNA TLR1_1 also inhibited LPS-stimulated Il6 release.

Since the efficiency of siRNA treatment could be confirmed, Il6 and TNFα release was measured in siRNA and NhhA-FL treated RAW264.7 cells.
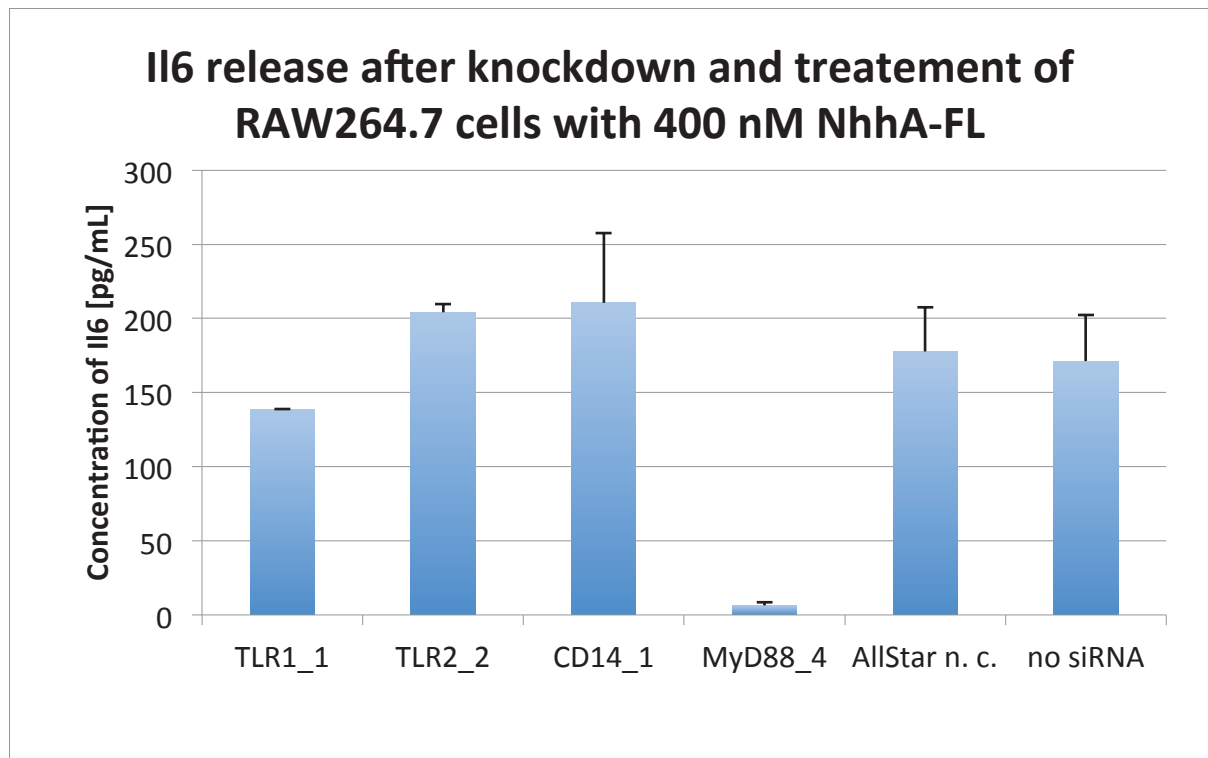
Fig. 27: Il6 release in cells treated with different siRNAs and NhhA-FL. The mean and standard deviation of three independent replicates is shown.

TNFα release after knockdown and treatement of RAW264.7 cells with 400 nM NhhA-FL
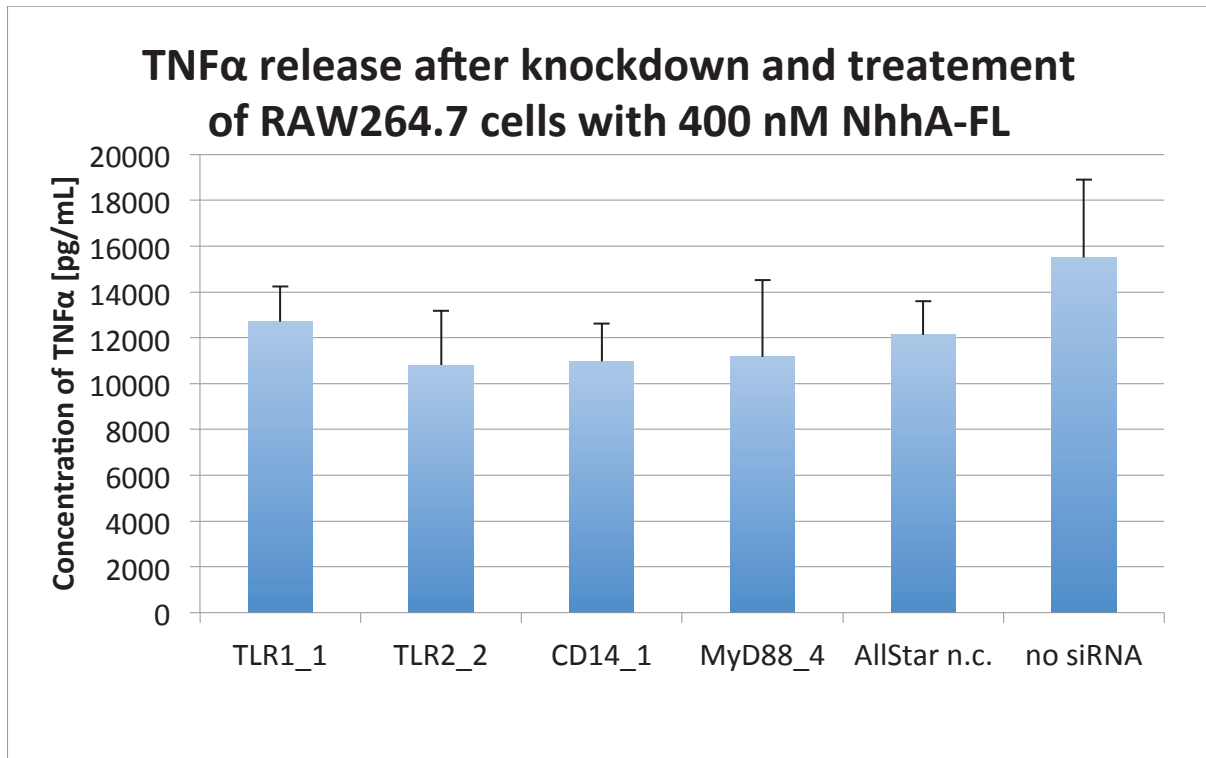
Fig. 28: TNFα release in cells treated with different siRNAs and NhhA-FL. The mean and standard deviation of three independent replicates is shown.

This data indicates that MyD88 is crucial for Il6 but not for TNFα release after NhhA-FL stimulation. NhhA-FL appears to activate signaling via two different pathways – one via TLR4 and MyD88, which is responsible for Il6 release and a completely different one, where at least TLR1, TLR2, TLR4, MyD88 and CD14 are not involved, which is responsible for TNFα release. A possible way could be through TLR3 and TRIF. For a greater overview of the TLR-pathway see the following figure.
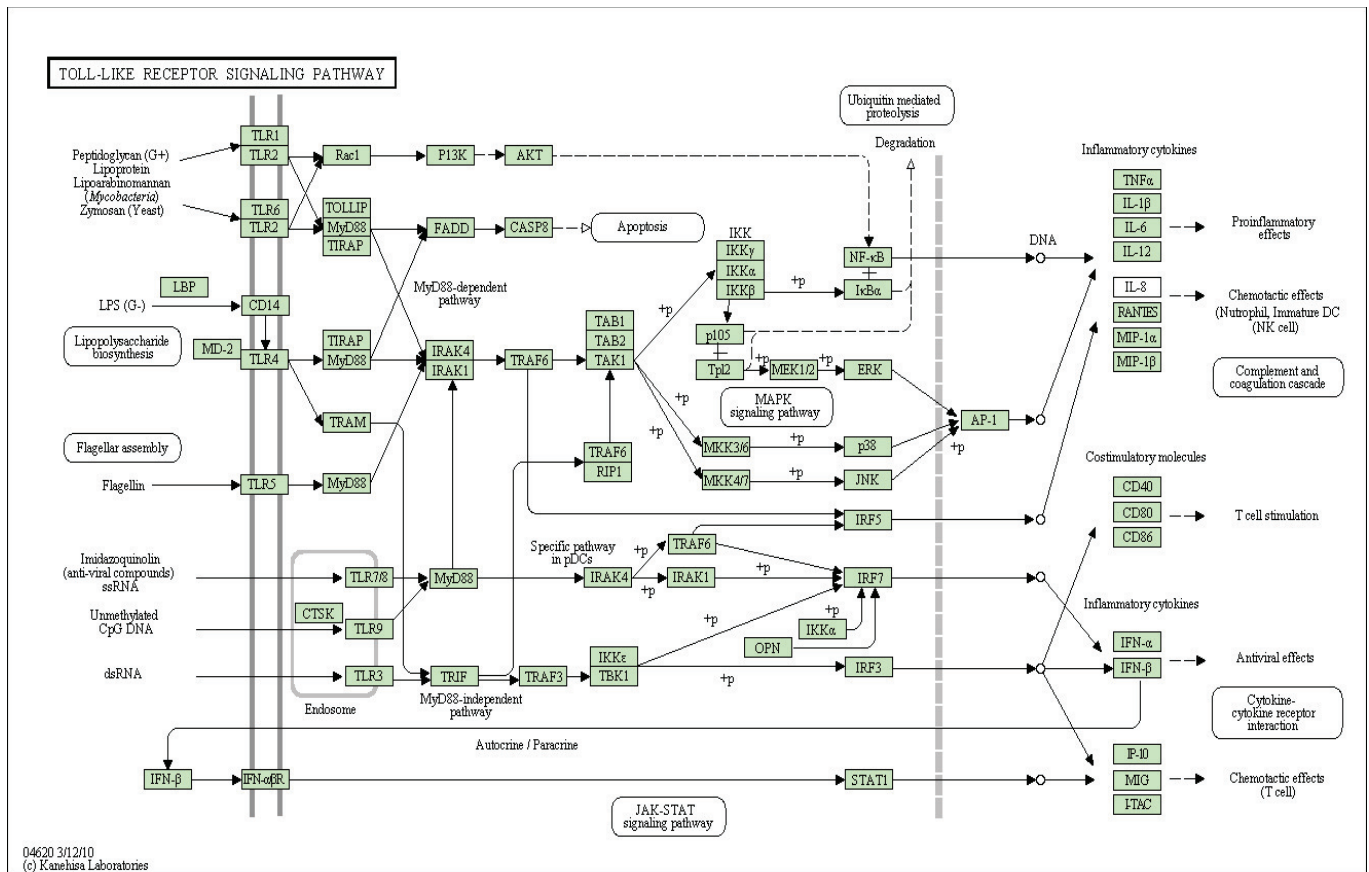
Fig. 29: Toll-like receptor pathway for mice from Kegg pathway database (*51*).

3.4. RNA isolation and RNA integrity

RNA integrity of isolated RNA was controlled with 1.2 % TAE agarose gel for all RNA samples used to generate data in 3.5. mRNA cytokine screen and verification. After staining with ethidiumbromide two distinct and intensive bands should be visible at approximately 4.9 and 1.9 kb against a light smear. The images show representative results after RNA isolation from RAW264.7 and differentiated THP-1 cells with and without NhhA-FL treatment. Additionally the concentration of RNA was measured with a nanodrop. This device also displays the absorbance ratio A_{260}/A_{280}. For pure RNA this ratio must be ≥2.0 and only samples, which fulfilled both requirements were used for further experiments. A proper RNA integrity is crucial for RT-qPCR results. With these quality controls, it was ensured that only samples with proper characteristics were used for subsequent experiments (*52, 53*).
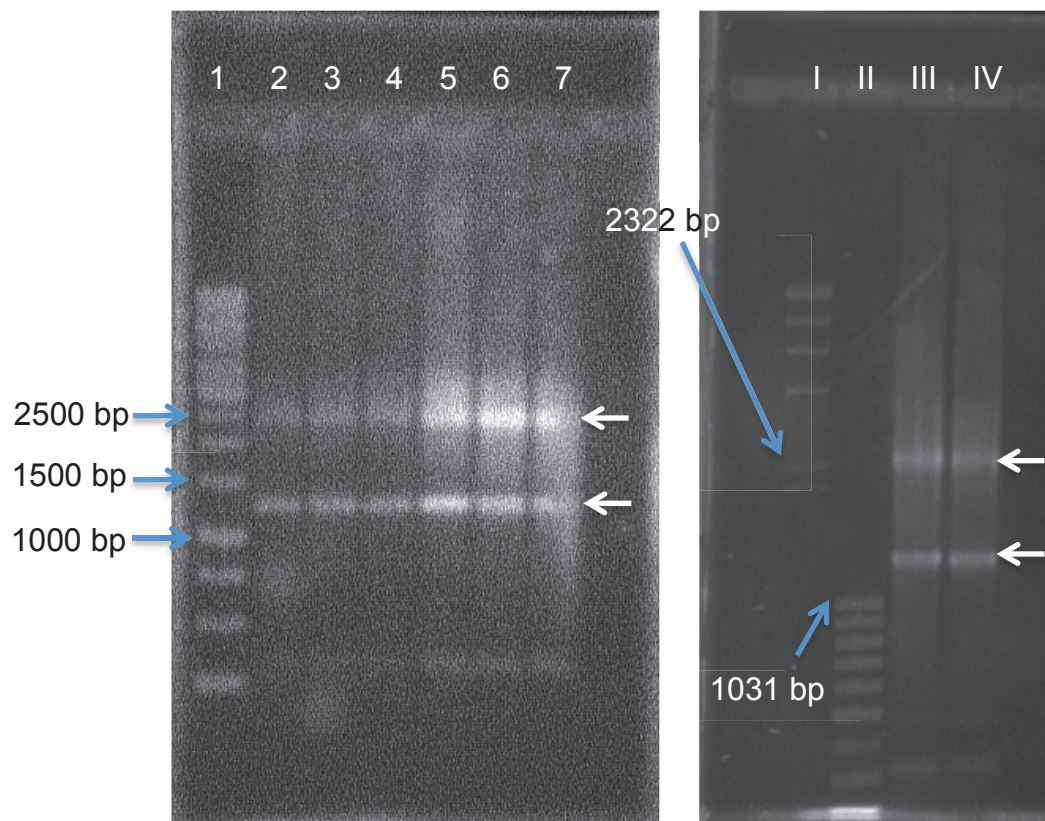
Fig. 30: Representative images of 1.2 % agarose gels stained with ethidiumbromide. 1: 1kb DNA ladder; 2: RNA from differentiated THP-1 cells treated with 400 nM NhhA-FL 1st replicate; 3: … 2nd aliquot; 4: … 3rd aliquot; 4: RNA from differentiated THP-1 cells 1st replicate; 5: … 2nd replicate; 6: …3rd replicate; I: λ/HindIII DNA Ladder; II: 100 bp DNA Ladder; III: RNA from RAW264.7 cells; IV: RNA from RAW264.7 cells treated with 400 nM NhhA-FL. Lanes 2, 3 and 4 are weaker than 5, 6 and 7 because less RNA was used. Since DNA ladders were used as marker, the values indicated have to be doubled to get the corresponding amount of bases.

3.5. mRNA cytokine screen and verification

Since NhhA-FL triggered Il6 and TNFα release further gene-regulatory events were investigated. Therefore, a qPCR array screen of 84 genes involved in TLR signaling was performed.

Results from the Toll-like receptor qPCR array are shown in figure 31. In the scatter plot a set of genes upregulated after NhhA-FL treatment could be observed.
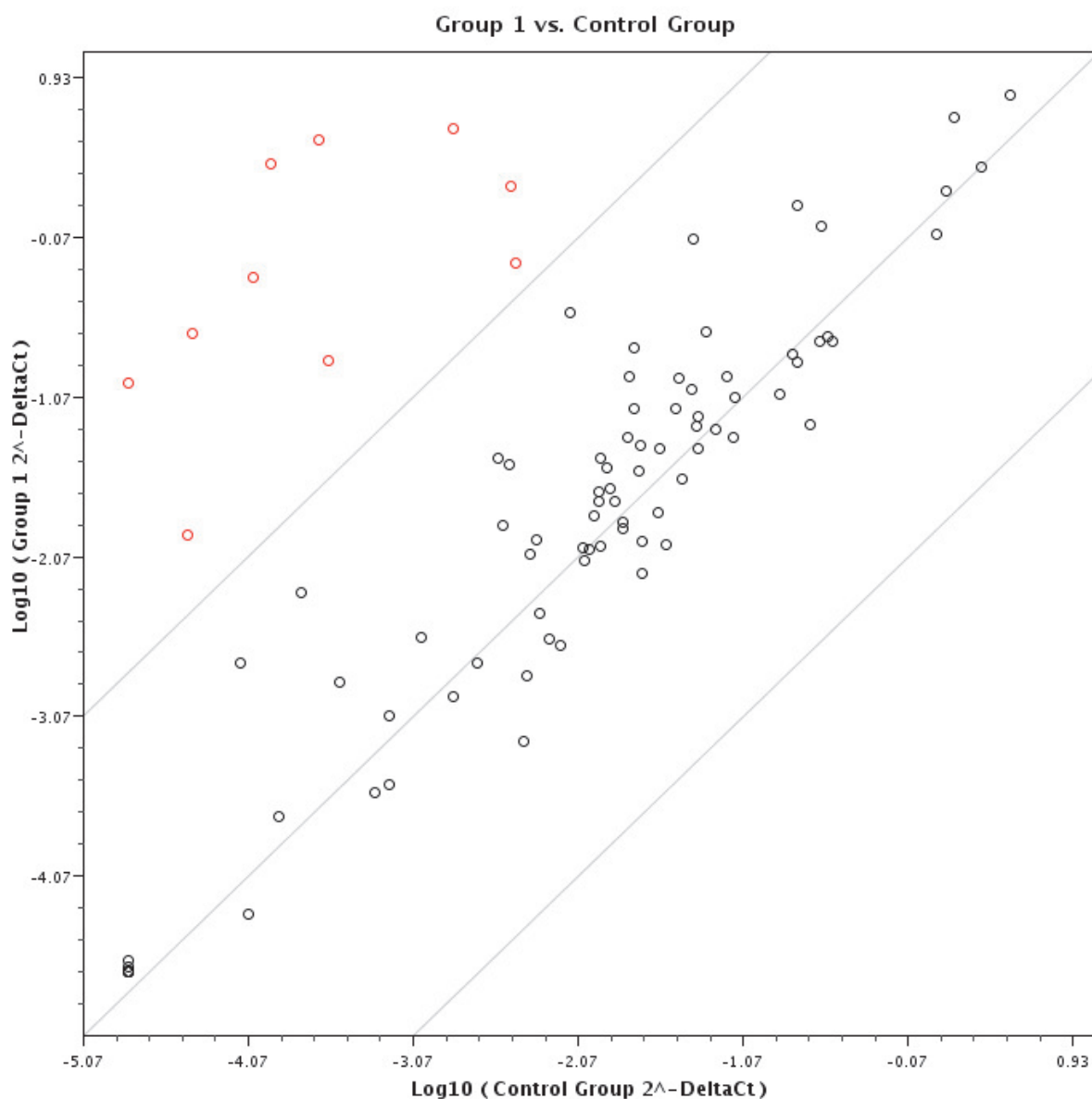
Fig. 31: Group 1 represents NhhA-FL treated RAW264.7 cells and control group represents untreated RAW 264.7 cells. All genes whose expressions are at least 100 fold upregulated are shown in red.

After obtaining these results, genes that were at least 100 fold upregulated were chosen for further investigation and verification in individual experiments. These genes and the results of the array are shown in the appendix. The genes that were at least 100 fold upregulated are shown in following table.

Table 5: Most upregulated genes (*54*, *55*)**.**

Gene name	Fold regulation	Gene function
Csf3	21056.8206	Anti-inflammatory cytokine; G-CSF; stimulates proliferation and differentiation of hematopoietic progenitor cells to neutrophils and granulocytes;

		induces colony formation
Il1b	15521.7112	Pro-inflammatory cytokine; enhances metabolism of arachidonic acid in inflammatory cells like fibroblasts; induces increased secretion of inflammatory proteins like neutral proteases, chemoattractant for leukocytes; activates oxidative metabolism in neutrophils
Il6	6617.1763	Pro-inflammatory cytokine; physiological mediator of the acute phase reactions; serves as marker to detect inflammation
Csf2	5412.2021	GM-CSF; responsible for differentiation of myoblasts and monoblasts; chemoattractant for neutrophils; enhances microbicidal activity, oxidative metabolism, phagocytotic activity and cytotoxicity of neutrophils and macrophages
Il1a	5227.8426	Pro-inflammatory cytokine; biologically equivalent to Il1b
Ptgs2	2743.8768	TIS10; encodes prostaglandin synthase 2
Il10	549.5093	Anti-inflammatory cytokine
Ccl2	534.4829	Pro-inflammatory chemokine; chemoattractant for monocytes
Ifnb1	324.4832	Pro-inflammatory cytokine; antiviral activity
Cxcl10	167.963	Pro-inflammatory chemokine; attracts natural killer cells

As shown in table 5, almost all genes which were at least 100 fold upregulated are pro-inflammatory cytokines or chemokines. NhhA-FL treated RAW264.7 cells were analyzed for the change in expression levels of these genes.
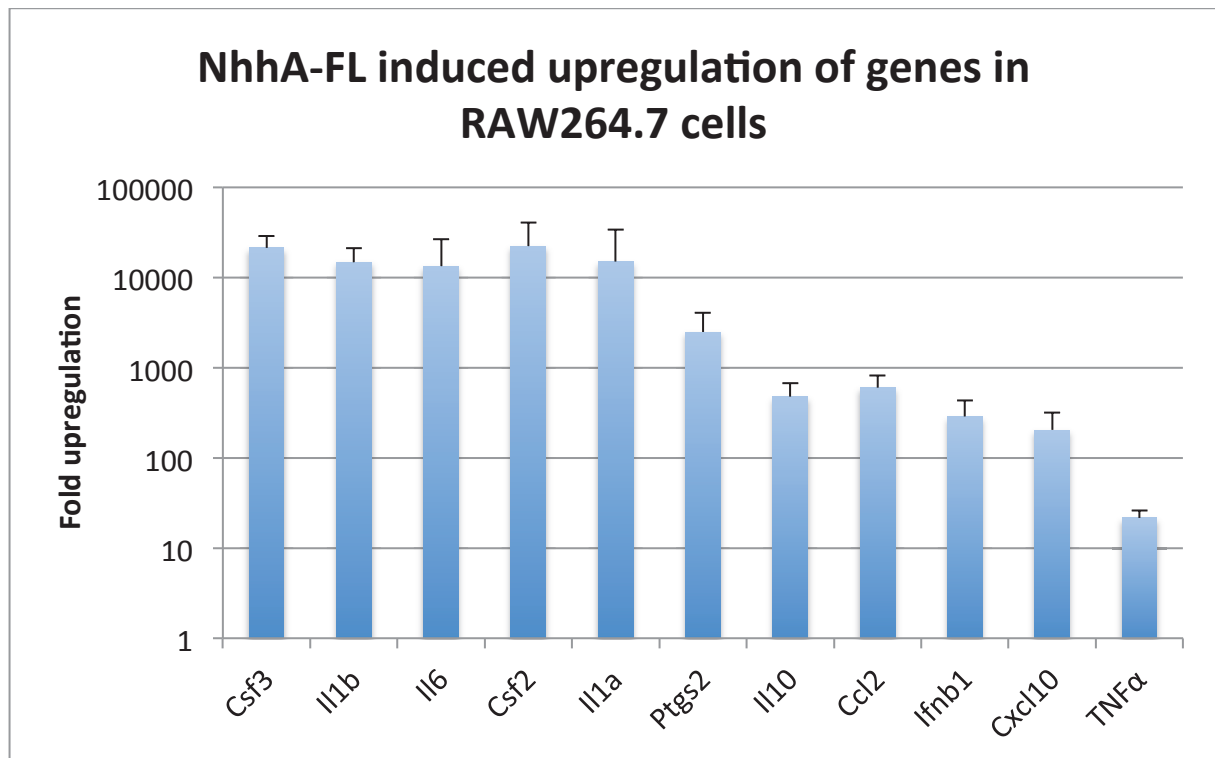
Fig. 32: Upregulation of genes after treatment of RAW264.7 cells with 400 nM NhhA-FL. The mean and standard deviation of three independent replicates is shown.

The results from the qPCR array could be validated by conventional qPCR. To confirm similar gene-regulatory events in human cells, the five most upregulated genes were selected (Csf3, Il1b, Il6, Csf2 and Il1a) and the changes in expression were measured in differentiated THP-1 cells. The THP-1 cell line is a human monocytic cell line, which can be differentiated to macrophage like cells by treating the cells with PMA (*44*). It is important to take into account that GAPDH is not stably expressed during monocyte differentiation to macrophages. Therefore, RPL37A was selected as reference gene (*47*).
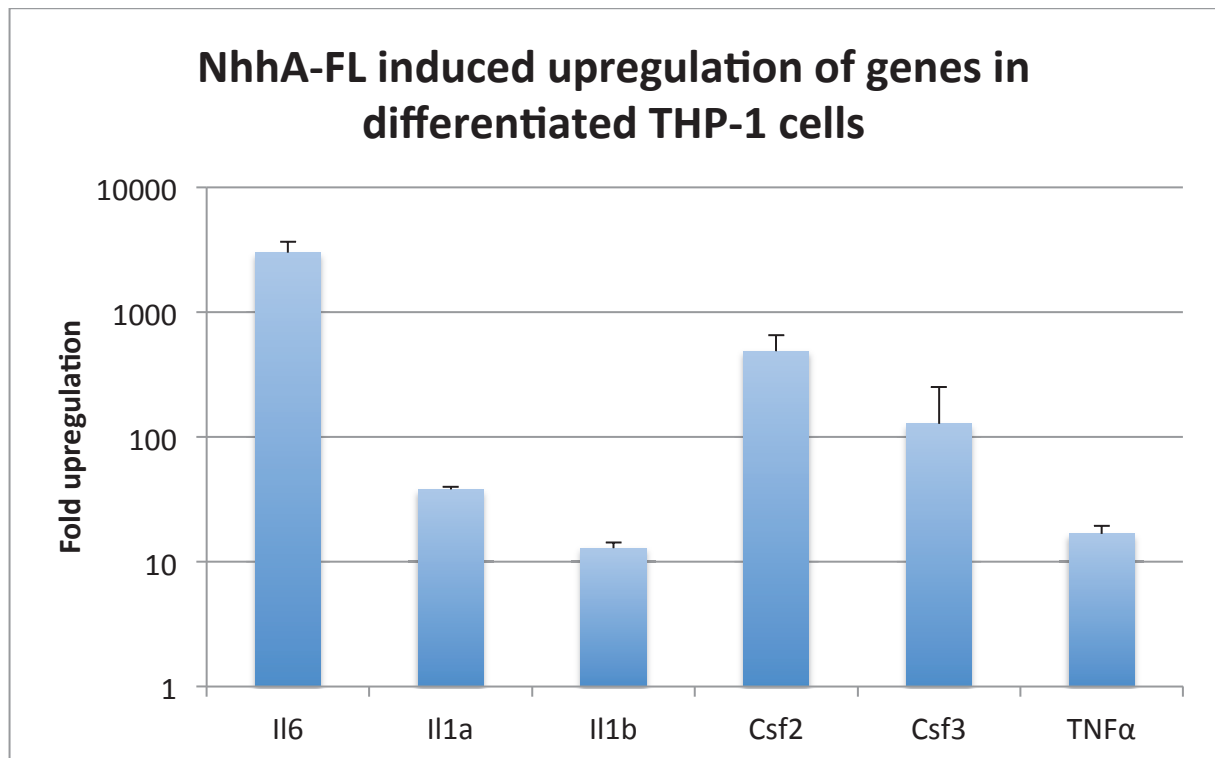
Fig. 33: Upregulation of genes after treatment of differentiated THP-1 cells with 400 nM NhhA-FL. The mean and standard deviation of three independent replicates is shown.

Additionally these results were compared with those obtained from differentiated cell treated with different NhhA fragments namely NhhA-FL, NhhA-FN, NhhA-FC and NhhA-FNAss. The excised amino acids in NhhA-FNAss were detected to be present in all other fragments. As it is shown in the figure, all fragments exhibit a potential of inducting proinflammatory cytokine expression, although fragments NhhA-FL and NhhA-FNAss have the highest potential. This finding was rather unexpected since it was assumed that the conserved motif might contribute to cytokine production and therefore, an excision of these amino acids might have abolished or at least diminished upregulation of the cytokines.
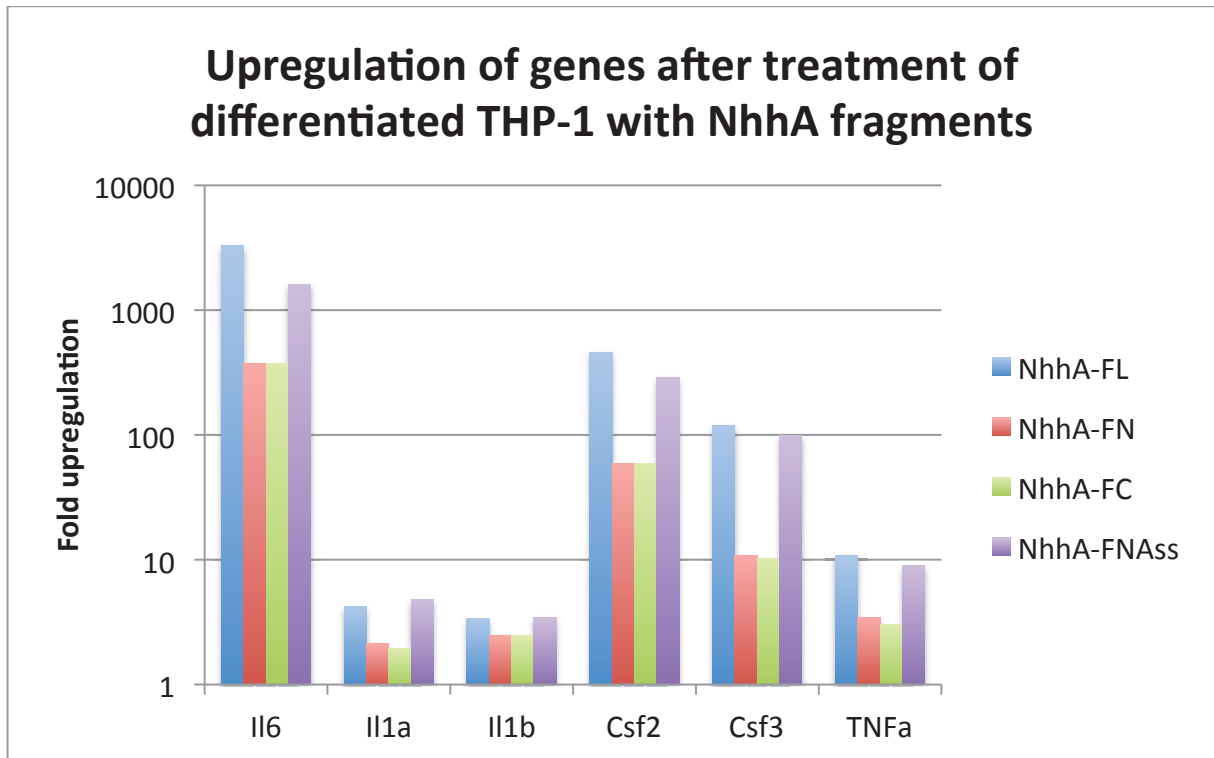
Fig. 34: Upregulation of genes after treatment of differentiated THP-1 cells with 400 nM of NhhA fragments.

Finally, comparing the potential of cytokine induction by NhhA-FL different concentrations of an outer membrane preparation of FAM20 was aimed at.
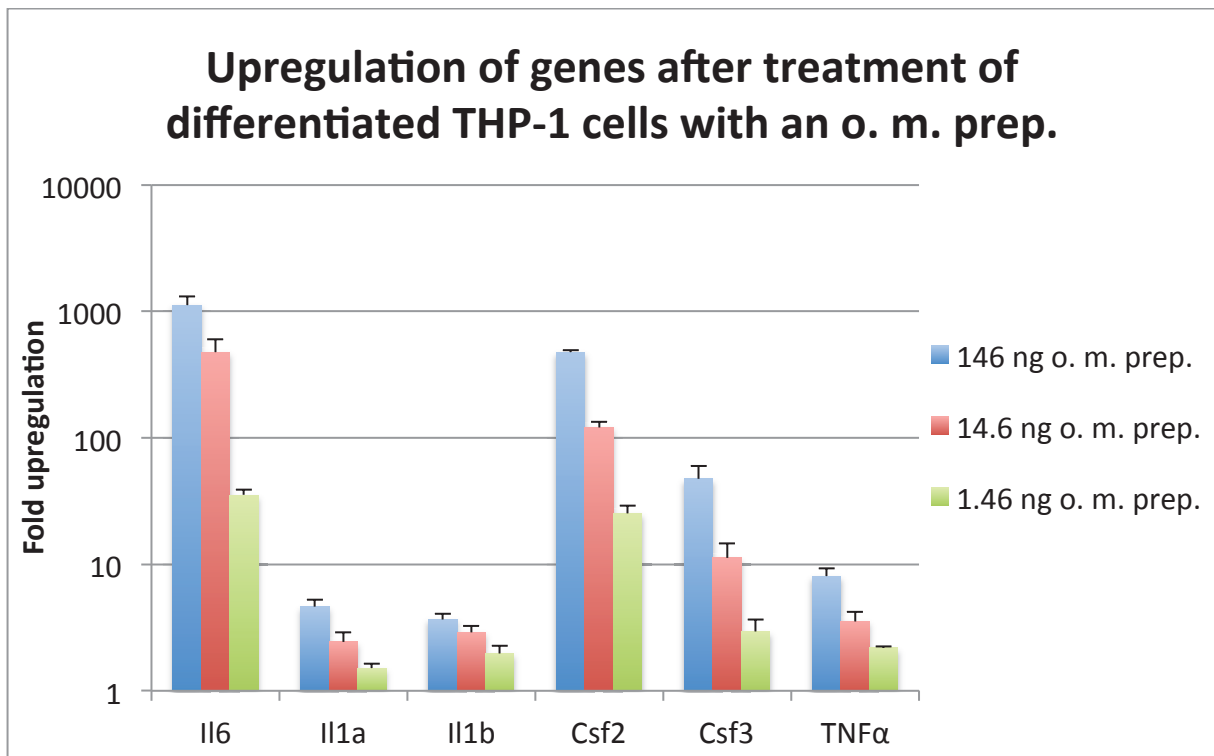
Fig. 35: Upregulation of genes after treatment of differentiated THP-1 cells with different amounts of an outer membrane preparation (o. m. prep.). The mean and standard deviation of three independent replicates is shown.

To strengthen the data on the signaling pathway achieved with the knockdown experiments, TLR4 was blocked by CLI-095 before NhhA-FL treatment of differentiated THP-1 cells. The, gene regulation of the five genes mentioned before was assessed, shown in fig. 36.

Upregulation of genes after inhibiton of TLR4 and treatment of differentiated THP-1 cells with NhhA-FL
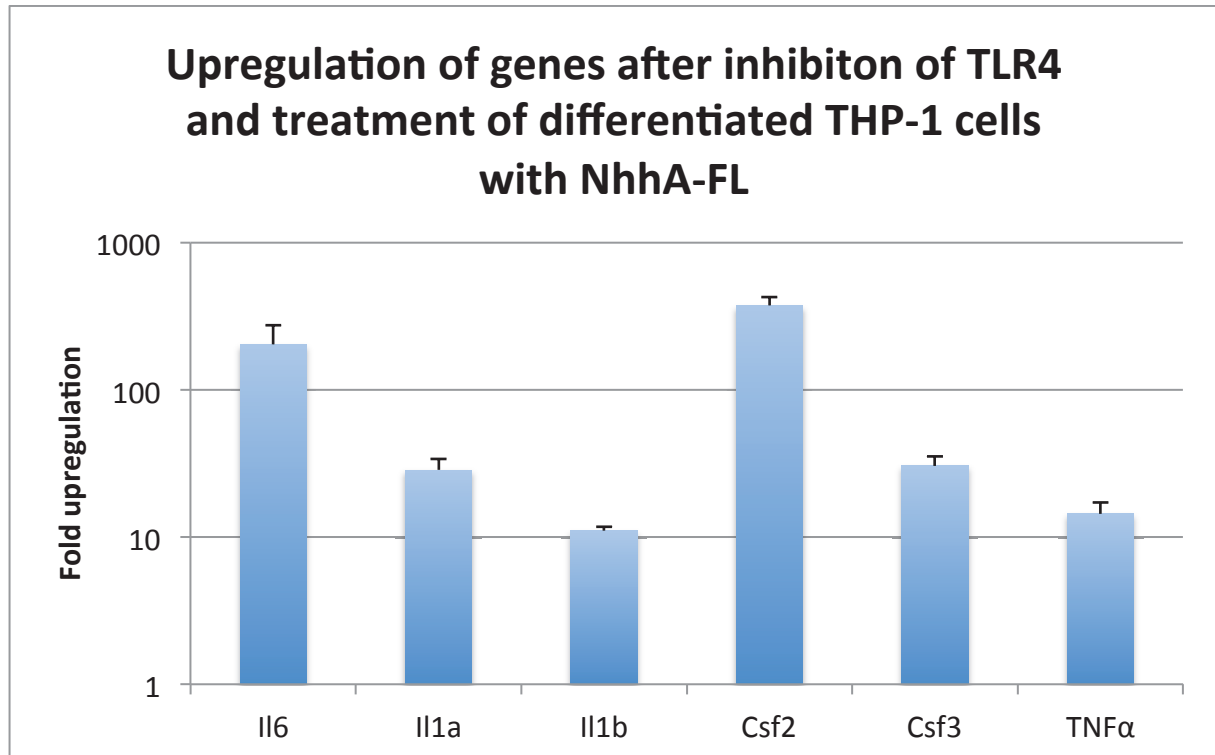
Fig. 36: Upregulation of genes after treatment of differentiated THP-1 cells with 1 μM CLI-095 and 400 nM NhhA-FL. The mean and normalized error of three independent replicates is shown.

This data shows that Il6 is potent downregulated upon blockade of TLR4 in differentiated THP-1 cells, which is consistent with the results obtained before in RAW264.7 cells (data not shown). Fig. 36 also shows, that the other genes are not affected by TLR4 blocking and therefore behave like TNFα. This is an additional indication that the results concerning the signaling cascade, obtained with the mouse cell line RAW264.7 also applies on the human cell line THP-1. Furthermore, it supports the theory that NhhA-FL has at least two different receptors and signals via two different pathways.

Overall, these results indicate that NhhA-FL is a very potent inducer of proinflammatory cytokines. The stunning fact is, that NhhA-FL has an even higher potential of inducing elevated expression levels of proinflammatory cytokines than the outer membrane preparation. This is remarkable since the outer membrane preparation should also contain LOS, which is known as one of the major inducers of inflammation (*10, 11*). However, stimulation with 400 nM NhhA-FL might not reflect

physiological concentrations of NhhA. In the experiments treatment of RAW264.7 cells with 400 nM NhhA-FL would result in approximately 36.1E16, treatment of THP-1 cells in approximately 48.2E16 molecules NhhA-FL per cell. As already mentioned before, for the apoptosis experiments, this seems to be very high. On the other hand, when the apoptosis results between NhhA-FL and FAM20 and FAM20ΔnhhA are compared, it shows that NhhA-FL induces apoptosis to the approximately same extent as FAM20 at the MOI=100. In the apoptosis experiments the ratio between NhhA-FL molecules and cells is even higher. Therefore, it seems that 400 nM NhhA-FL is a concentration that is in general biologically relevant. Thus, it was consistent to use the same concentration for the cytokine measurements.

Despite the overall consistency of the data obtained from the cytokine experiments RAW264.7 and THP-1 cells, differences in the fold upregulation of the cytokines tested can be detected. This represents a general difficulty with research on *N. meningitidis* since animal models are only limited due to the ecological niche of meningococci. This data was not confirmed in macrophages isolated from humans, since it is still not entirely known why some people are susceptible to invasive disease and others are not. Therefore, data obtained from these experiments would not have been representative since the results strongly depend on the donor.

3.6. Western blot

Another point of interest was to investigate how the chosen time points for the apoptosis experiments and RNA isolation correlated to binding of NhhA-FL to cells. The following figure shows a western blot, where NhhA-FL was detected bound on RAW264.7 cells at different timepoints.
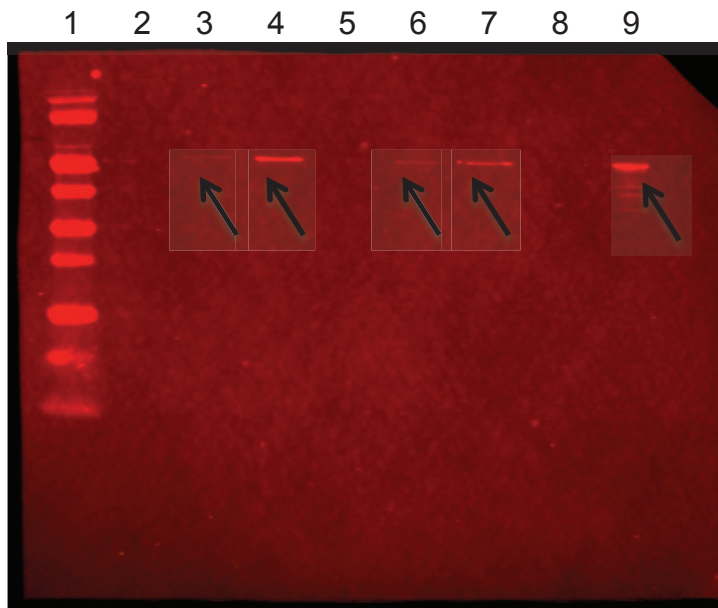
Fig. 37: 1: Marker; 2: RAW264.7 + 10 nM NhhA-FL, 6 h; 3: RAW264.7 + 100 nM NhhA-FL, 6 h; 4: RAW264.7 + 400 nM NhhA-FL, 6 h; 5: RAW264.7 + 10 nM NhhA-FL 21 h; 6: RAW264.7 + 100 nM NhhA-FL 21 h; 7: RAW264.7 + 400 nM NhhA-FL 21 h; 8: RAW264.7 cells control; 9: 400 nM NhhA-FL

After 21 h NhhA-FL is still bound to the cells, indicating that NhhA-FL interacts with the cells during the whole time period of the apoptosis- and RNA-related experiments performed.

4. Conclusion

The aim of this project was to assess the apoptotic and inflammatory potential of NhhA. Therefore, a truncated version of NhhA was generated. This fragment called NhhA-FL lacks the leader peptide and the translocator domain but contains a his-tag for protein purification. When RAW264.7 mouse macrophages and differentiated human THP-1 cells were treated with this truncated NhhA-FL, apoptosis was induced through a yet to be determined pathway. Additionally, induction of apoptosis upon treatment with NhhA-FL was also observed in undifferentiated THP-1 cells. The results obtained from macrophages or macrophage-like cells treated with *N. meningitidis* FAM20 or FAM20ΔnhhA confirm the results obtained from cells treated with NhhA-FL.

Moreover, it was shown that NhhA-FL has a high inflammatory potential. The results show that Il6 and TNFα protein levels are significantly upregulated after NhhA-FL treatment. Furthermore, it has been proven that NhhA-FL signals at least through two different pathways. Signaling through TLR4 and the MyD88 dependent pathway induces Il6 release. This was proven by abolished Il6 expression when MyD88 was knocked down. TNFα was not affected by knocking down any of the receptors and adapter proteins tested (TLR1, TLR2, CD14 and MyD88). Subsequently, these results in mouse macrophages not only suggest a signaling through two different pathways but also that NhhA-FL might be able to bind to at least two different receptors. Nevertheless, signaling converges at NFκB in mouse macrophages, since inhibition of NFκB abolishes both, Il6 and TNFα release (unpublished data). In human THP-1 cells, inhibition of TLR4 with CLI-095 also decreased Il6 mRNA levels in contrast to the other genes tested, which were not affected. These results, additionally, strongly support the aforementioned conclusion, which is based on the results of a different cell line.

The screening for other highly upregulated members of the TLR-pathway in mouse macrophages resulted in 10 mRNAs which are more than 100fold upregulated upon NhhA-FL treatment. These mRNA encoded the cytokines Csf3, Il1b, Il6, Csf2, Il1a, Ptgs2, Il10, Ccl2, Ifnb1 and Cxcl10. Subsequently, the regulation of the five most upregulated cytokines in RAW264.7 cells was also tested in differentiated THP-1 cells. The results obtained from these experiments show some big differences. The mRNA levels of these cytokines are still highly upregulated but not even closely as high as in RAW264.7 cells. Nevertheless, the expression of the tested proinflammatory cytokines after NhhA-FL treatment of THP-1 cells was generally

even higher than after treatment with an outer membrane preparation of FAM20. This is remarkable because the outer membrane preparation should contain LOS and lipid A, both major inducers of inflammation. Since the outer membrane preparation was heated over night for 60 °C it is reasonable to assume that the only inducer of cytokines are LOS and lipid A, respectively, due to their heat resistance (*10*).

In the end, it is noteworthy to mention that an upregulation of mRNA levels is not necessarily connected to an upregulation of protein levels. Further experiments like ELISAs are necessary to prove this.

5. Appendix

5.1. Toll-like receptor pathway screen results

Table 6: Gene expression changes in RAW264.7 cells after NhhA-FL treatment.

Fold change	Gene	Fold change	Gene	Fold change	Gene
21056.8206	Csf3	2.3983	Tlr1	1.3679	Ifng
15521.7112	Il1b	2.3166	Irak2	1.3398	Traf6
6617.1763	Il6	2.2847	Tlr6	1.2675	Rela
5412.2021	Csf2	2.1916	Tnfrsf1a	1.1423	Hsp90ab1
5227.8426	Il1a	2.117	Tbk1	1.1188	Tlr7
2743.8768	Ptgs2	2.0591	Myd88	1.0512	Mapk8
549.5093	Il10	2.0307	RTC	1.0014	Gapdh
534.4829	Ccl2	1.8947	Jun	-1.0483	Mapk8ip3
324.4832	Ifnb1	1.8557	Actb	-1.0629	Chuk
167.963	Cxcl10	1.7195	RTC	-1.0703	Ube2v1
38.6394	Tnfaip3	1.6958	Nfkbil1	-1.1157	Ikbkb
28.4824	Cd86	1.6841	Tlr2	-1.1235	Tlr8
24.1174	Lta	1.6609	Ly96	-1.1392	Map3k7
19.3197	Tnf	1.6495	RTC	-1.1471	Tlr4
12.7462	Cd80	1.6155	Il2	-1.1712	Nfrkb
10.0005	Tlr3	1.5713	PPC	-1.2294	Nr2c2
9.3957	Peli1	1.5605	PPC	-1.2816	Map2k3
7.5266	Nfkbia	1.5605	Ppara	-1.3086	Ly86
6.6438	Clec4e	1.5497	Tirap	-1.3086	Elk1
4.6012	Nfkbib	1.4969	Tollip	-1.3086	Casp8
4.5065	Ticam1	1.456	Il1r1	-1.3547	Hprt1
4.353	Nfkb1	1.4359	PPC	-1.3928	Btk
3.9231	Cebpb	1.426	Map2k4	-1.4025	Hspd1
3.896	Rel	1.426	Hspa1a	-1.5562	Hras1
3.1866	Eif2ak2	1.4064	Agfg1	-1.567	Gusb
3.0568	Irf1	1.3679	Tlr5	-1.5999	Hmgb1
2.9938	Cd14	1.3679	Muc13	-1.611	Tradd
2.8324	Ripk2	1.3679	MGDC	-1.7029	Pglyrp1
2.8324	Nfkb2	1.3679	Il12a	-1.7752	Fadd

Fold change	Gene
-1.9159	Irf3
-1.9426	Irak1
-2.2161	Map3k1
-2.6907	Ube2n
-2.7856	Mapk9
-2.8245	Il6ra
-3.1123	Ticam2
-3.8317	Fos
-6.7646	Tlr9

5.2. Primer sequences for qPCR

Table 7: Mouse primers for qPCR experiments.

Primer	Direction	Sequence (5'→3')	Application	E
GAPDH	forward	CAACTTTGTCAAGCTCATTTCCTG	qPCR	1.88
	reversed	CCTCTCTTGCTCAGTGTCCTT	qPCR	
TLR1	forward	CCGTGATGCACAGCTCCTTGGTT	qPCR	n. d.
	reversed	TGCCTCTGCTCGCCTGAGTTCT	qPCR	
TLR2	forward	GAGGACTCCTAGGCTCCGGGCA	qPCR	n. d.
	reversed	GACTGCCGTCCAACCTTCACCA	qPCR	
CD14	forward	ACAGGGGCTGCCAAATTGGTCG	qPCR	n. d.
	reversed	AGCACACGCTCCATGGTCGGTA	qPCR	
MyD88	forward	CCCCCTAGGACAAACGCCGGA	qPCR	n. d.
	reversed	GGCAGGACGTCACGGTCGGA	qPCR	
Csf3	forward	TCCAGGCCAGCGGCTCGGTG	qPCR	2.00
	reversed	TGTCTGCTGCAGGGCCTGGC	qPCR	
Il1b	forward	GCCTCGTGCTGTCGGACCCATA	qPCR	1.97
	reversed	TGCAGGGTGGGTGTGCCGTCTT	qPCR	
Il6	forward	AGCTGGAGTCACAGAAGGAGTGGC	qPCR	2.00
	reversed	GGCATAACGCACTAGGTTTGCCGAG	qPCR	
Csf2	forward	GCCATCAAAGAAGCCCTGAA	qPCR	2.00
	reversed	GCGGGTCTGCACACATGTTA	qPCR	
Il1a	forward	GGAGAAGACCAGCCCGTGTTGCT	qPCR	1.88

	reversed	CCGTGCCAGGTGCACCCGACTT	qPCR	
Ptgs2	forward	GCCAGCTCCACCGCCACCACT	qPCR	2.00
	reversed	GAGCCCCAGGGCAGCGCAGA	qPCR	
Il10	forward	TGCACCCACTTCCCAGTCGGCCA	qPCR	2.00
	reversed	TGGCTGAAGGCAGTCCGCAGCTC	qPCR	
Ccl2	forward	TTGCCGGCTGGAGCATCCACGT	qPCR	2.00
	reversed	AGTAGCAGCAGGTGAGTGGGGCG	qPCR	
Ifnb1	forward	GCCTGGATGGTGGTCCGAGCA	qPCR	2.00
	reversed	TACCAGTCCCAGAGTCCGCCTCT	qPCR	
Cxcl10	forward	TCCGGAAGCCTCCCCATCAGCACC	qPCR	2.00
	reversed	TGCAGCGGACCGTCCTTGCGA	qPCR	
TNFα	forward	TCCCAGGTTCTCTTCAAGGGA	qPCR	2.00
	reversed	GGTGAGGAGCACGTAGTCGG	qPCR	

Table 8: Human primers for qPCR experiments.

Primer	Direction	Sequence (5'→3')	Application	E
RPL37A	forward	ATTGAAATCAGCCAGCACGC	qPCR	1.97
	reversed	AGGAACCACAGTGCCAGATCC	qPCR	
Csf3	forward	TCTGAGTTTCATTCTCCTGCCTG	qPCR	2.00
	reversed	ATTTACCTATCTACCTCCCAGTCCAG	qPCR	
Il1b	forward	TCCCCAGCCCTTTTGTTGA	qPCR	1.97
	reversed	TTAGAACCAAATGTGGCCGTG	qPCR	
Il6	forward	GGCACTGGCAGAAAACAACC	qPCR	2.00
	reversed	GCAAGTCTCCTCATTGAATCC	qPCR	
Csf2	forward	CTCAGAAATGTTTGACCTCCAG	qPCR	1.88
	reversed	TGACAAGCAGAAAGTCCTTCAG	qPCR	
Il1a	forward	CGCCAATGACTCAGAGGAAGA	qPCR	2.00
	reversed	AGGGCGTCATTCAGGATGAA	qPCR	
TNFα	forward	CCTGCCCCAATCCCTTTATT	qPCR	2.00
	reversed	CCCTAAGCCCCCAATTCTCT	qPCR	

5.3. Formula

5.4. List of tables

5.5. List of figures

5.6. List of References

1. Hill, D. J., Griffiths, N. J., Borodina, E., and Virji, M. (2010) Cellular and molecular biology of Neisseria meningitidis colonization and invasive disease., *Clinical Science 118*, 547-564.

2. Caugant, D. A., and Maiden, M. C. J. (2009) Meningococcal carriage and disease—Population biology and evolution, *Vaccine 27*, B64-B70.

3. Stephens, D. S., Greenwood, B., and Brandtzaeg, P. (2007) Epidemic meningitis, meningococcaemia, and Neisseria meningitidis., *Lancet 369*, 2196-210.

4. derstandard.at. http://derstandard.at/1301873791778/Oberoesterreich-Schuelerin-starb-vermutlich-an-Meningokokken-Infektion. Accessed on November, 4, 2011

5. Tzeng, Y. L., and Stephens, D. S. (2000) Epidemiology and pathogenesis of Neisseria meningitidis., *Microbes and Infection / Institut Pasteur 2*, 687-700.

6. Rosenstein, N. E., Perkins, B. A., Stephens, D. S., Popovic, T., and Hughes, J. M. (2001) Meningococcal Disease, *The New England Journal of Medicine 344*, 1378-1388.

7. Maclennan, J., Kafatos, G., Neal, K., Andrews, N., Cameron, J. C., Roberts, R., Evans, M. R., Cann, K., Baxter, D. N., and Maiden, M. C. J. (2006) Social Behavior and Meningococcal Carriage in British Teenagers, *Emerging Infectious Diseases 12*, 950-957.

8. Frosch, M., Weisgerber, C., and Meyert, T. F. (1989) Molecular characterization and expression in Escherichia coli of the gene complex encoding the polysaccharide capsule of Neisseria meningitidis group B, *Proc. Natl. Acad. Sci. USA 86*, 1669-1673.

9. Swartley, J. S., Liu, L.-jun, Miller, Y. K., Martin, L. E., Edupuganti, S., and Stephens, D. S. (1998) Characterization of the Gene Cassette Required for Biosynthesis of Capsule of Serogroup A Neisseria meningitidis, *Journal of Bacteriology 180*, 1533-1539.

10. Brandtzaeg, P., Bjerre, A., Ovstebo, R., Brusletto, B., Joo, G. B., and Kierulf, P. (2001) Invited Review: Neisseria meningitidis lipopolysaccharides in human pathology, *Journal of Endotoxin Research 7*, 401-420.

11. Plant, L., Sundqvist, J., Zughaier, S., Lo, L., Stephens, D. S., and Jonsson, A.-beth. (2006) Lipooligosaccharide Structure Contributes to Multiple Steps in the Virulence of Neisseria meningitidis, *Infection and Immunity 74*, 1360-1367.

12. Verheul, A. F. M., Snippe, H., and Poolman, J. T. (1993) Meningococcal lipopolysaccharides: virulence factor and potential vaccine component., *Microbiological Reviews 57*, 34-49.

13. Devoe, I. W., and Gilchrist, J. E. (1973) Release of endotoxin in the form of cell wall blebs during in vitro growht of Neisseria meningitidis, *The Journal of Experimental Medicine 138*, 1156-1167.

14. Zughaier, S. M., Tzeng, Y. L., Zimmer, S. M., Datta, A., Carlson, R. W., and Stephens, D. S. (2004) Neisseria meningitidis lipooligosaccharide structure-dependent activation of the macrophage CD14/Toll-like receptor 4 pathway, *Infection and Immunity 72*, 371-380.

15. Zughaier, S. M., Zimmer, S. M., Datta, A., Carlson, R. W., and Stephens, D. S. (2005) Differential Induction of the Toll-Like Receptor 4–MyD88-Dependent and -Independent Signaling Pathways by Endotoxins, *Infection and Immunity 73*, 2940-2950.

16. Pelicic, V. (2008) MicroReview Type IV pili : e pluribus unum ?, *Molecular Microbiology 68*, 827-837.

17. Carbonnelle, E., Hill, D. J., Morand, P., Griffiths, N. J., Bourdoulous, S., Murillo, I., Nassif, X., and Virji, M. (2009) Meningococcal interactions with the host, *Vaccine 27S*, B78–B89.

18. Orihuela, C. J., Mahdavi, J., Thornton, J., Mann, B., Wooldridge, K. G., Abouseada, N., Oldfield, N. J., Self, T., and Tuomanen, E. I. (2009) Laminin receptor initiates bacterial contact with the blood brain barrier in experimental meningitis models, *The Journal of Clinical Investigation 119*, 1638-1646.

19. Källström, H., Liszewski, M. K., Atkinson, J. P., and Jonsson, a B. (1997) Membrane cofactor protein (MCP or CD46) is a cellular pilus receptor for pathogenic Neisseria., *Molecular Microbiology 25*, 639-47.

20. Kirchner, M., Heuer, D., and Meyer, T. F. (2005) CD46-independent binding of neisserial type IV pili and the major pilus adhesin, PilC, to human epithelial cells, *Infection and Immunity 73*, 3072-3082.

21. Vries, F. P. de, Cole, R., Dankert, J., Frosch, M., and Putten, J. P. van. (1998) Neisseria meningitidis producing the Opc adhesin binds epithelial cell proteoglycan receptors., *Molecular Microbiology 27*, 1203-1212.

22. Malorny, B., Morelli, G., and Kusecek, B. (1998) Sequence diversity, predicted two-dimensional protein structure, and epitope mapping of neisserial Opa proteins, *Journal of Bacteriology 180*, 1323-30.

23. Virji, M., Makepeace, K., Ferguson, D. J. P., and Watt, S. M. (1996) Carcinoembryonic antigens (CD66) on epithelial cells and neutrophils are receptors for Opa proteins of pathogenic neisseriae, *Molecular Microbiology 22*, 941-950.

24. Virji, M., Makepeace, K., and Moxon, E. R. (1994) Distinct mechanisms of interactions of Opc-expressing meningococci at apical and basolateral surfaces of human endothelial cells; the role of integrins in apical interactions, *Molecular Microbiology 14*, 173-184.

25. Virji, M., Watt, S. M., Barker, S., Makepeace, K., and Doyonnas, R. (1996) The N-domain of the human CD66a adhesion molecule is a target for Opa proteins of Neisseria meningitidis and Neisseria gonorrhoeae, *Molecular Microbiology 22*, 929-939.

26. Lehmann, A. K., Halstensen, A., Aaberge, I. S., Holst, J., Michaelsen, T. E., Sørnes, S., Wetzler, L. M., and Guttormsen, H. K. (1999) Human Opsonins Induced during Meningococcal Disease Recognize Outer Membrane Proteins PorA and PorB, *Infection and Immunity 67*, 2552-2560.

27. Massari, P., Ram, S., Macleod, H., and Wetzler, L. M. (2003) The role of porins in neisserial pathogenesis and immunity, *Trends in Microbiology 11*, 87-93.

28. Müller, A., Günther, D., Brinkmann, V., Hurwitz, R., Meyer, T. F., and Rudel, T. (2000) Targeting of the pro-apoptotic VDAC-like porin (PorB) of Neisseria gonorrhoeae to mitochondria of infected cells, *EMBO Journal 19*, 5332-5343.

29. Müller, A., Günther, D., Düx, F., Naumann, M., Meyer, T. F., and Rudel, T. (1999) Neisserial porin (PorB) causes rapid calcium influx in target cells and induces apoptosis by the activation of cysteine proteases, *EMBO Journal 18*, 339-352.

30. Müller, A., Rassow, J., Grimm, J., Machuy, N., Meyer, T. F., and Rudel, T. (2002) VDAC and the bacterial porin PorB of Neisseria gonorrhoeae share mitochondrial import pathways, *EMBO Journal 21*, 1916-1929.

31. Massari, P., Ho, Y., and Wetzler, L. M. (2000) Neisseria meningitidis porin PorB interacts with mitochondria and protects cells from apoptosis, *Proc. Natl. Acad. Sci. USA 97*, 9070-9075.

32. Trivedi, K., Tang, C. M., and Exley, R. M. (2011) Mechanisms of meningococcal colonisation., *Trends in Microbiology 19*, 456-63.

33. Merz, A. J., Enns, C. A., and So, M. (1999) Type IV pili of pathogenic Neisseriae elicit cortical plaque formation in epithelial cells, *Molecular Microbiology 32*, 1316-1332.

34. Mikaty, G., Soyer, M., Mairey, E., Henry, N., Dyer, D., Forest, K. T., Morand, P., Guadagnini, S., Prévost, M. C., Nassif, X., and Duménil, G. (2009) Extracellular Bacterial Pathogen Induces Host Cell Surface Reorganization to Resist Shear Stress, *PLoS Pathogens 5*, e1000314. doi:101371/journal.ppat.1000314.

35. Eugène, E., Hoffmann, I., Pujol, C., Couraud, P.-O., Bourdoulous, S., and Nassif, X. (2002) Microvilli-like structures are associated with the internalization of virulent capsulated Neisseria meningitidis into vascular endothelial cells., *Journal of Cell Science 115*, 1231-1241.

36. Scarselli, M., Serruto, D., Montanari, P., Capecchi, B., Adu-Bobie, J., Veggi, D., Rappuoli, R., Pizza, M., and Aricò, B. (2006) Neisseria meningitidis NhhA is a multifunctional trimeric autotransporter adhesin., *Molecular Microbiology 61*, 631-644.

37. Sutherland, T. C., Quattroni, P., Exley, R. M., and Tang, C. M. (2010) Transcellular passage of Neisseria meningitidis across a polarized respiratory epithelium., *Infection and Immunity 78*, 3832-47.

38. Thompson, M. J., Ninis, N., Perera, R., Mayon-White, R., Phillips, C., Bailey, L., Harnden, A., Mant, D., and Levin, M. (2006) Clinical recognition of meningococcal disease in children and adolescents., *Lancet 367*, 397-403.

39. US Patent # 7,947,291. Modified surface antigen. http://patents.com/us-7947291.html. Accessed on November, 5, 2011

40. Peak, I., Srikhanta, Y., Dieckelmann, M., Moxon, E., and Jennings, M. (2000) Identification and characterisation of a novel conserved outer membrane protein from Neisseria meningitidis, *FEMS Immunology and Medical Microbiology 28*, 329-334.

41. Pizza, M., Scarlato, V., Masignani, V., Giuliani, M., Aricò, B., Comanducci, M., Jennings, G., Baldi, L., Bartolini, E., Capecchi, B., Galeotti, C., Luzzi, E., Manetti, R., Marchetti, E., Mora, M., Nuti, S., Ratti, G., Santini, L., Savino, S., Scarselli, M., Stroni, E., Peijun Z, Broeker, M., Hundt, E., Knapp, B., Blair, E., Mason, T., Tettelin, H., Hood, D., Jeffries, A., Saunders, N., Granoff, D., Venter, J., Moxon, E. R., Grandi, G., and Rappuoli, R. (2000) Identification of Vaccine Candidates Against Serogroup B Meningococcus by Whole-Genome Sequencing, *Science 287*, 1816-1820.

42. Scarselli, M., Rappuoli, R., and Scarlato, V. (2001) A common conserved amino acid motif module shared by bacterial and intercellular adhesins: bacterial adherence mimicking cell–cell recognition?, *Microbiology 147*, 250-252.

43. Sjölinder, H., Eriksson, J., Maudsdotter, L., Aro, H., and Jonsson, A.-B. (2008) Meningococcal Outer Membrane Protein NhhA Is Essential for Colonization and Disease by Preventing Phagocytosis and Complement Attack, *Infection and Immunity 76*, 5412-5420.

44. Daigneault, M., Preston, J. A., Marriott, H. M., Whyte, M. K. B., and Dockrell, D. H. (2010) The Identification of Markers of Macrophage Differentiation in PMA-Stimulated THP-1 Cells and Monocyte-Derived Macrophages, *PLoS One 5*, e8668.

45. Meyer, M., Essack, M., Kanyanda, S., and Rees, J. G. (2008) A low-cost flow cytometric assay for the detection and quantification of apoptosis using an anionic halogenated fluorescein dye, *BioTechniques 45*, 317–320.

46. Evrogen Technologies: RNA electrophoresis protocol. http://www.evrogen.com/technologies/RNA-electrophoresis.shtml. Accessed on June, 14, 2011.

47. Maeß, M. B., Sendelbach, S., and Lorkowski, S. (2010) Selection of reliable reference genes during THP-1 monocyte differentiation into macrophages, *BMC Molecular Biology 11*, 90.

48. Akira, S., and Takeda, K. (2004) Toll-Like Receptor Signalling, *Nature Reviews Immunology 4*, 499-511.

49. Zhu, J., and Mohan, C. (2010) Toll-like receptor signaling pathways-- therapeutic opportunities., *Mediators of Inflammation 2010*, 781235.

50. Chen, K., Huang, J., Gong, W., Iribarren, P., Dunlop, N. M., and Wang, J. M. (2007) Toll-like receptors in inflammation, infection and cancer., *International Immunopharmacology 7*, 1271-1285.

51. TLR-pathway of Kegg database. http://www.genome.jp/kegg-bin/show_pathway?org_name=mmu&mapno=04620&mapscale=&show_description=hide. Accessed on November, 6, 2011.

52. Fleige, S., and Pfaffl, M. W. (2006) RNA integrity and the effect on the real-time qRT-PCR performance., *Molecular Aspects of Medicine 27*, 126-139.

53. Hoffmann-Rohrer, U. W., and Kruchen, B. (Eds.). Lab FAQS 3rd Edition. Roche.

54. Dinarello, C. a. (2000) Proinflammatory Cytokines, *Chest 118*, 503-508.

55. Cope with cytokines. http://www.copewithcytokines.org. Accessed on November, 8, 2011.